Distribution of copper-binding ligands in Fram Strait and influences from the Greenland Shelf (GEOTRACES GN05)

Veronica Arnone, J. Magdalena Santana-Casiano, Melchor González-Dávila, Géraldine Sarthou, Stephan Krisch, Pablo Lodeiro, Eric Achterberg, Aridane González

HAL Id: hal-04317676

https://hal.univ-brest.fr/hal-04317676

Submitted on 28 Dec 2023

Distribution of copper-binding ligands in Fram Strait and influences from the Greenland Shelf (GEOTRACES GN05)

Veronica Arnone [a], J. Magdalena Santana-Casiano [a], Melchor González-Dávila [a], Géraldine Sarthou [b], Stephan Krisch [c], Pablo Lodeiro [d], Eric P. Achterberg [c], Aridane G. González [a,*]

[a] Instituto de Oceanografía y Cambio Global, IOCAG, Universidad de Las Palmas de Gran Canaria, ULPGC, Spain
[b] Univ Brest, CNRS, IRD, Ifremer, LEMAR, F-29280 Plouzane, France
[c] GEOMAR Helmholtz Centre for Ocean Research Kiel, 24148 Kiel, Germany
[d] Department of Chemistry, Physics, Environmental and Soil sciences, University of Lleida-AGROTECNIO-CERCA Center, Rovira Roure 191, 25198, Lleida, Spain

HIGHLIGHTS

- Cu complexation was measured for the first time in the Fram Strait region.
- Cu-binding ligand concentrations and binding strength varied longitudinally in the Fram Strait.
- More than 99 % of dCu was organically complexed by strong ligands.
- On the Greenland shelf the Transpolar Drift and the coastal processes were the main sources of Cu ligands.

GRAPHICAL ABSTRACT
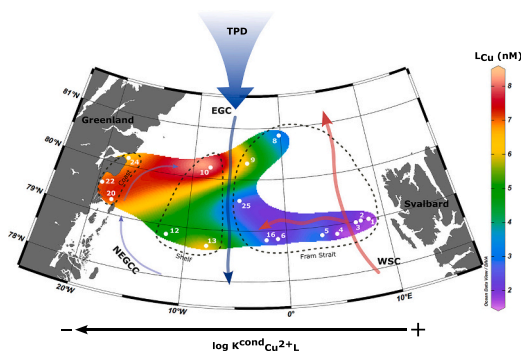
ARTICLE INFO

ABSTRACT

The Fram Strait represents the major gateway of Arctic Ocean waters towards the Nordic Seas and North Atlantic Ocean and is a key region to study the impact of climate change on biogeochemical cycles. In the region, information about trace metal speciation, such as copper, is scarce. This manuscript presents the concentrations and conditional stability constants of copper-binding ligands (L_{Cu} and log K^{cond}_{Cu2+L}) in the water column of Fram Strait and the Greenland shelf (GEOTRACES cruise GN05). Cu-binding ligands were analysed by Competitive Ligand Exchange-Adsorptive Cathodic Stripping Voltammetry (CLE-ACSV) using salicylaldoxime (SA) as competitive ligand. Based on water masses and the hydrodynamic influences, three provinces were considered (coast, shelf, and Fram Strait) and differences were observed between regions and water masses. The strongest variability was observed in surface waters, with increasing L_{Cu} concentrations (mean values: Fram Strait = 2.6 ± 1.0 nM; shelf = 5.2 ± 1.3 nM; coast = 6.4 ± 0.8 nM) and decreasing log K^{cond}_{Cu2+L} values (mean values: Fram Strait = 15.7 ± 0.3; shelf = 15.2 ± 0.3; coast = 14.8 ± 0.3) towards the west. The surface L_{Cu} concentrations obtained above the Greenland shelf indicate a supply from the coastal environment to the Polar Surface Water (PSW) which is an addition to the ligand exported from the central Arctic to Fram Strait. The significant differences (in

* Corresponding author.
E-mail address: aridane.gonzalez@ulpgc.es (A.G. González).

terms of L_{Cu} and log K_{Cu2+L}^{cond}) between shelf and coastal samples were explained considering the processes which modify ligand concentrations and binding strengths, such as biological activity in sea-ice, phytoplankton bloom in surface waters, bacterial degradation, and meltwater discharge from 79NG glacier terminus. Overall, the ligand concentration exceeded those of dissolved Cu (dCu) and kept the free copper (Cu^{2+}) concentrations at femtomolar levels (0.13–21.13 fM). This indicates that Cu^{2+} toxicity limits were not reached and dCu levels were stabilized in surface waters by organic complexes, which favoured its transport to the Nordic Seas and North Atlantic Ocean and the development of microorganism.

1. Introduction

The Arctic region is highly vulnerable to the impact of climate change, with the warming of this polar area being two to three times faster than the global average (IPCC, 2022). The decrease of sea-ice coverage, associated with regional warming, increases light penetration and enhances phytoplankton growth in nutrient-rich waters (Arrigo et al., 2008). The decreasing sea-ice coverage changes the carbon uptake (Cai et al., 2010), modifies the ocean currents (Wang et al., 2020) and decreases (−15 % per decade) the transport of ice-rafted materials from the Siberian shelves towards the Nordic Seas (Krumpen et al., 2019). Furthermore, the increase in riverine runoff (Feng et al., 2021; Peterson et al., 2002) and the permafrost thawing (Schuur et al., 2015, 2013) causes a rapid increase in organic matter discharge (Frey and McClelland, 2009; Stedmon et al., 2011). These inputs contain trace metals (Charette et al., 2020; Guieu et al., 1996) and metal-binding ligands (Slagter et al., 2017), essential for numerous biogeochemical processes, including the phytoplankton growth (Twining and Baines, 2013). Trace metals bioavailability is determined by speciation, which is strongly influenced by the formation of complexes with organic molecules, referred to as ligands, that constitute a heterogeneous group of compounds with distinct functional groups. Ligands are involved in trace metal assimilation and distribution by limiting scavenging processes and influencing dissolution and precipitation rates. The consequences of climate change are still largely unknown but could impact the biogeochemical cycles of bio-essential trace metals, such as copper (Maldonado et al., 2006; Peers et al., 2005; Sunda, 1989), including their organic speciation.

Copper (Cu) is an essential micronutrient required for numerous metabolic functions in phytoplankton development (Twining and Baines, 2013). The free cupric ion (Cu^{2+}), on the other hand, is toxic at relatively high concentrations and could inhibit phytoplankton growth rates (Brand et al., 1986). The organic speciation of Cu in seawater, its bioavailability and toxicity, is strongly controlled by the formation of complexes with organic Cu-binding ligands (L_{Cu}). These ligands are classified based on the conditional stability constant (K_{Cu2+L}^{cond}, Buck and Bruland, 2005) into strong (L_1, log K_{Cu2+L}^{cond} = 13–16) and weak ligand classes (L_2, log K_{Cu2+L}^{cond} = 11–13), which provide information about the binding strength but not about molecular characterization of the organic compounds. Nevertheless, different functional groups have been identified as Cu-binding ligands, such as exopolysaccharides (log K_{Cu2+L}^{cond} < 8, Lombardi et al., 2005), humic substances (log K_{Cu2+L}^{cond} = 10–12, Kogut and Voelker, 2001; Whitby and van den Berg, 2015), thiols (log K_{Cu2+L}^{cond} = 11–16, Walsh and Ahner, 2013) and methanobactins (log K_{Cu2+L}^{cond} > 14, Choi et al., 2006). However, there is a lack of information on the oceanic distribution and nature of Cu speciation, particularly in the Arctic region with limited data on Cu-binding ligand concentrations reported for Canadian Arctic waters (Nixon et al., 2019), the sub-arctic North Pacific (Moffett and Dupont, 2007; Whitby et al., 2018; Wong et al., 2021) and the North Atlantic Ocean (Gourain, 2020; Kramer, 1986).

In the Arctic Ocean, the supply of metal-binding ligands is largely related to terrestrial sources that introduce Dissolved Organic Matter (DOM) throughout river discharges (Amon, 2003; Benner et al., 2005; Guéguen et al., 2007; Opsahl et al., 1999). About 10 % of global riverine discharge of freshwater arrives in the Arctic (Benner et al., 2005). Freshwater and shelf-derived material from the Eurasian region, including metal-binding ligands (Ardiningsih et al., 2020; Krisch et al., 2022; Laglera et al., 2019; Slagter et al., 2019, 2017), are transported towards the central Arctic by the Transpolar Drift (TPD, Gordienko and Laktionov, 1969) and subsequently through Fram Strait and towards the Nordic Seas and North Atlantic Ocean (Ardiningsih et al., 2020; Williford et al., 2022). About 18–26 % of the terrigenous DOM that reaches the Arctic is exported to the Nordic Seas by the TPD, which is associated with the East Greenland Current (EGC, Benner et al., 2005). This export potentially impacts the global carbon cycle, the cycling of other elements, and biological production. Additional sources of organic matter and metal-binding ligands in the Arctic region are sediments (Davis and Benner, 2005; Goñi et al., 2013), phytoplankton or microbial production (Benner et al., 2005), and sea-ice melt (Charette et al., 2020). Considering that Arctic waters spend 2-3 years travelling from the Siberian shelves to the Fram Strait (Pfirman et al., 1997), during this transit the organic matter is subject to modifications related to sea-ice melt or formation, shelf-sea interactions, flocculation, biological DOM degradation, photooxidation and sediment release from ice (Charette et al., 2020; Slagter et al., 2017).

Within the high-latitude region, the Fram Strait is the major gateway of water from the Arctic to the Atlantic Ocean (Rudels, 2019). It is a key region to understand the impact of climate change on biogeochemical cycles. The region is a source of dissolved trace metals (Krisch et al., 2022), metal-binding ligands (Ardiningsih et al., 2020) and DOM (Granskog et al., 2012) to the Nordic seas and towards the North Atlantic Ocean, due to a pronounced Arctic export. In addition, the Arctic surface water transports large amounts of dissolved trace metals (Gerringa et al., 2021) and DOM (Amon, 2003; Davis and Benner, 2005; Guéguen et al., 2007; Opsahl et al., 1999) with fluvial origin. The Fram Strait also receives waters from the Atlantic Ocean that have lower concentrations of Fe-binding ligands (Ardiningsih et al., 2020) and dissolved trace metal than Arctic surface waters (Krisch et al., 2022), and DOM related to marine origin (Granskog et al., 2012). The western region of Fram Strait receives large volumes of freshwater due to the melting along the coastal margins of the Greenland Ice Sheet which can be an important source of metal-binding ligands to the ocean. The Nioghalvfjerdsfjorden Glacier (79NG), located in the study area, is one of the major outlets of the North-East Greenland Ice Stream (NEGIS), which drains 12 % of the Greenland Ice Sheet area (Rignot and Mouginot, 2012). The meltwater flux corresponds to 14.2 ± 0.96 km^3 year^{-1} (Wilson et al., 2017) and contributes (up to 13 %) to the coloured DOM (CDOM) concentrations in coastal waters (Stedmon et al., 2011) and Fe-binding ligands (Ardiningsih et al., 2020). However, the contribution of dissolved micronutrients is lower than 2 % of the total micronutrient transported across the Fram Strait (Krisch et al., 2022).

In this study, data of Cu-binding ligand concentrations and conditional stability constants (L_{Cu} and log K_{Cu2+L}^{cond}) in Fram Strait and over the northeast Greenland shelf are presented and related to the water masses in the region, in order to identify possible sources of Cu-binding ligands. This study will provide critical information on the controls of Cu cycling in a region that is experiencing rapid changes.

2. Methods

2.1. Sampling

Samples were collected during a GEOTRACES cruise (GN05) on the RV Polarstern (PS100) during the boreal summer (from July 22nd to September 1st, 2016). The water column was sampled along the northeast Greenland shelf, near the 79NG glacier terminus and across the Fram Strait (Fig. 1). Details about the cruise can be found in the expedition report (Kanzow, 2016). Seawater for trace metal analysis was taken following GEOTRACES sampling procedure (Cutter et al., 2010) with a trace metal clean rosette and the GO-FLO bottles (Ocean Test Equipment). Right after recovery, the rosette was transferred into an over-pressured clean container (class 100) and the water was filtered

(Acropak 0.8/0.2 μm pore size) into 125 mL low-density polyethylene (LDPE) bottles. The bottles were cleaned following GEOTRACES protocols (Cutter et al., 2010) and, after sampling, stored at -20 °C.

Conductivity, temperature and depth were measured with a Sea-Bird CTD (SBE 911plus) installed on the trace metal clean rosette frame. Macronutrient data (NO_3^-, NO_2^-, PO_4^{3-}, $Si(OH)_4$) obtained from the trace metal clean rosette were reported by Graeve et al. (2019).

2.2. Analysis of Cu-binding ligands by CLE-ACSV

The dCu concentrations have been measured and reported by Krisch et al. (2022). They were measured by high-resolution inductively coupled plasma-mass spectrometry (HR-ICP-MS) following solid-phase extraction after preconcentration using an automated SeaFAST system
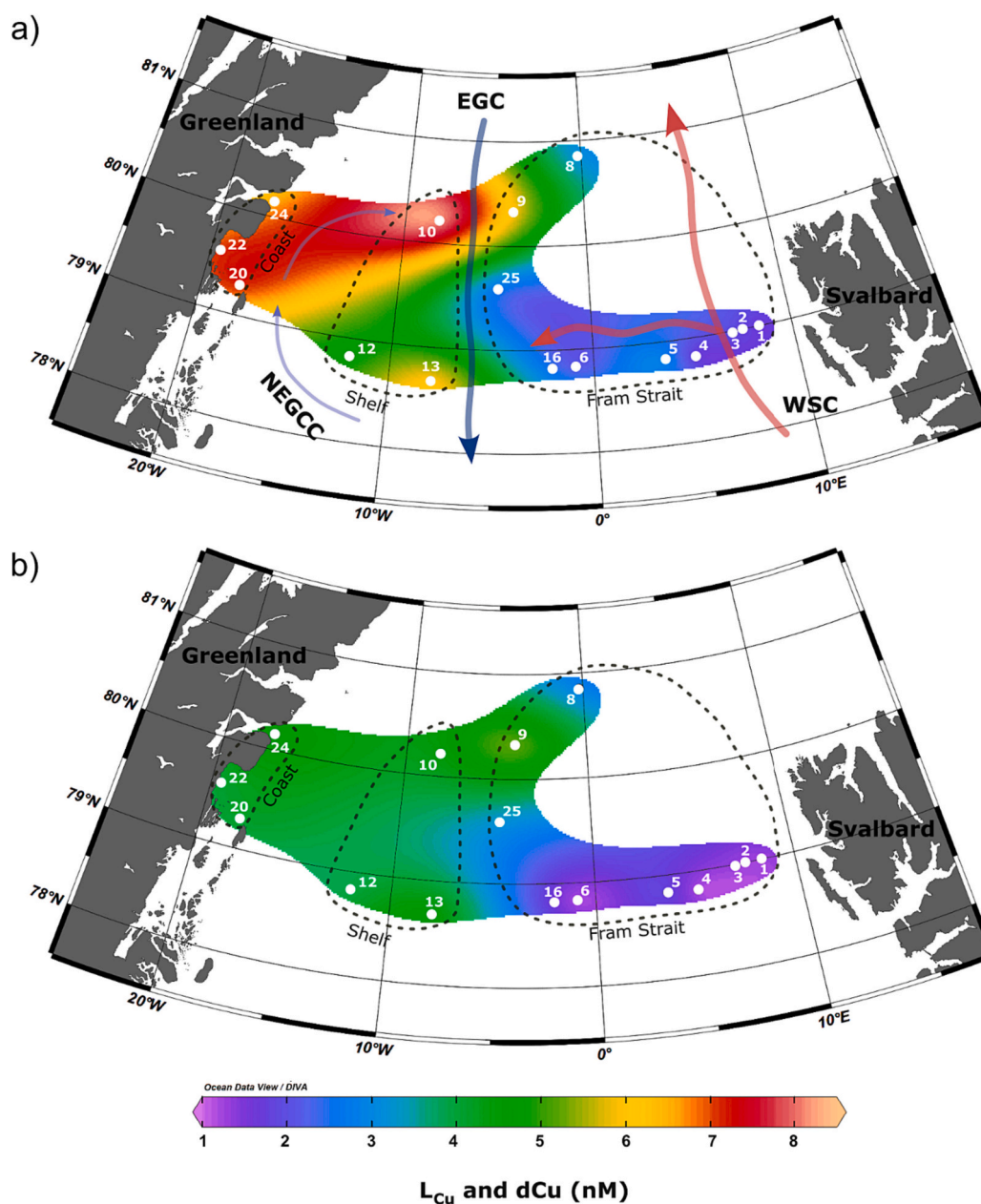
Fig. 1. Map of the study area and surface distribution of a) Cu-binding ligands (L_{Cu}, in nM) and b) dissolved Cu (dCu, in nM). The information about dCu has been reported by Krisch et al. (2022). Station location during GEOTRACES expeditions GN05 (2016) in Fram Strait and schematic flowpaths of major currents are shown. The West Spitsbergen Current (WSC) was depicted in red and the East Greenland Current (EGC) in blue. Above the Greenland shelf, thin blue arrows indicate the circulation of the North-East Greenland Coastal Current (NEGCC). Three zones have been differentiated in the study, enclosed by dashed line and from east to west denoted as: Fram Strait, shelf and coast.

(SC-4 DX SeaFAST pico; ESI) (Rapp et al., 2017).

The concentration of Cu-binding ligands (L_{Cu}) and the conditional stability constants (K^{cond}_{Cu2+L}) were determined using the Competitive Ligand Exchange-Adsorptive Cathodic Stripping Voltammetry (CLE-ACSV) with SA as competitive ligand (Campos and van den Berg, 1994). Accordingly, 1 M boric acid was prepared in 0.3 M ammonia as buffer (pH 8.2), 0.01 M solution of salicylaldoxime (SA) was prepared in 0.1 M suprapure HCl and Cu stock solutions (Fluka), were used. Possibly remaining metals were removed from the buffer solution by adding 100 μM of MnO_2, stirred overnight and filtered through an acid-clean 0.45 μm filter (van den Berg, 1982). To guarantee the chemical properties, both SA and Cu stock solutions were prepared every other week and together with the buffer were kept in the fridge (at 8 °C and darkness) when they were not in use. Briefly, 10 mL samples were pipetted into 10 PTFE vials (22 mL volume), 100 μL of buffer (final concentration 10^{-2} M) and different concentrations of Cu were added (from 0 to 10 or 15 nM). A few samples were analysed with higher Cu addition, up to 20 nM, but no differences were found in the Cu-binding ligand determination. After a 1 h equilibration period, 10 μL of SA (final concentration 10 μM) was added and left to equilibrate overnight. The measurements were performed using a Hanging Mercury Drop Electrode (VA663 stand Metrohm), an Ag/AgCl reference electrode with a KCl salt bridge (3 M) and a glassy carbon counter electrode. Following 120 s nitrogen gas purge, a deposition potential of − 0.2 V was applied for 180 s. After 10 s of equilibration, a differential pulse scan was applied from −0.2 to −0.5 V, with a step potential 3 mV, modulation amplitude 49.95 mV, interval time 0.1 s and modulation time of 0.05 s. Data fitting was performed with PromCC software (Omanović et al., 2015) using the "complete fitting" for one ligand (Supplementary material Fig. S1). For each titration curve, the sensitivity was determined by internal calibration, from the last titration points (4 or 5) which presented linearity. This method assumes that in the linear portion of the titration curve all ligands were titrated. In some samples, to ensure that all ligands had been fully titrated, two Cu additions were made to the last titration point (with 4 or 8 nM of Cu) and measured immediately. These additions were not used during data treatment.

The side reaction coefficient for CuSA (α_{CuSA}) and the inorganic metal ($\alpha_{Cu'}$) was calculated for each seawater sample to consider the salinity variability (Campos and van den Berg, 1994). The α_{CuSA}, represents the centre of the detection window (D) and its value is a function of the SA concentration and the salinity (S), that affects the conditional stability constants for CuSA 1:1 and 1:2 complexes (log K^{cond}_{CuSA}, log $\beta^{cond}_{Cu(SA)_2}$), as expressed below:

$$\alpha_{CuSA} = K^{cond}_{CuSA} \bullet [SA] + \beta^{cond}_{Cu(SA)_2} \bullet [SA]^2 = D \quad (1)$$

$$log K^{cond}_{CuSA} = 10.12 - 0.37 \bullet log S \quad (2)$$

$$log \beta^{cond}_{Cu(SA)_2} = 15.78 - 0.53 \bullet log S \quad (3)$$

The $\alpha_{Cu'}$ is defined by the stability constants (β^{cond}_{CuXi}) of the complexes formed between Cu and the major seawater ions (X_i), and the acidity Cu constant ($\beta^{cond}_{Cu(OH)i}$) at seawater ionic strength, as defined by:

$$\alpha_{Cu'} = 1 + \sum \left(\beta^{cond}_{CuX_i} \bullet [X]^i \right) + \sum \left(\beta^{cond}_{Cu(OH)_i} / [H^+]^i \right) \quad (4)$$

In this case, given the salinity range (29.87–35.14) the log α_{CuSA} varied between 5.10 and 5.14 while the $\alpha_{Cu'}$ ranged from 28 to 30. This variability did not produce important modifications on the detection windows.

2.3. Statistical analysis

Statistical analysis was applied to determine whether there are significant differences in physical properties (temperature, salinity), macronutrient concentrations (NO_3^-, NO_2^-, PO_4^{3-}, $Si(OH)_4$), dCu concentrations and parameters associated with Cu-binding ligands (concentrations of L_{Cu}, eL_{Cu}, Cu' and Cu^{2+}, as well as log K^{cond}_{Cu2+L} and log α_{Cu2+L}) between regions and water masses. Since the variables displayed a non-normal distribution and heteroscedasticity, a Kruskal-Wallis test (Kruskal and Wallis, 1952) was applied to determine significant differences between regions (Supplementary material Table S1) and water masses (Supplementary material Table S2). For parameters that presented significant differences (p-value<0.05), a Conover test (Conover and Iman, 1979) was applied to elucidate which groups (regions or water mass) were different.

3. Results

3.1. Hydrographic description

The main current and water mass distributions in the region have been described elsewhere (Laukert et al., 2017; Rudels et al., 2005) and shortly summarised here (Figs. 1 and 2). Different water masses were defined based on potential temperatures (θ) and potential densities (referred to 0 and 500 dbar of pressure, σ_0 and σ_{500} respectively). The relatively warm (potential temperature θ > 2 °C) and saline (S > 35) Atlantic Water (AW, 27.7 < σ_0 < 27.97) is carried northwards by the West Spitsbergen Current (WSC) in the upper 500 m depth on the eastern part of the Fram Strait. On the western side, the East Greenland Current (EGC) flows southward and brings cold (θ ≤ 0 °C) and less saline (S < 34.5) Polar Surface Water (PSW, σ_0 ≤ 27.7) to the Atlantic Ocean, above 200 m depth (Laukert et al., 2017). The interaction of both current systems within the Fram Strait creates the Recirculated Atlantic Water (RAW, θ > 0 °C, σ_0 > 27.97, σ_0 < 30.444), which flows southward with the WSC at ~500 m (Rudels et al., 2005). Mostly on the western Fram Strait, the Arctic Atlantic Water (AAW, 0 < θ ≤ 2 °C, 27.7 < σ_0 < 29.97) flows southward between 150 and 300 m depth. In Fram Strait, the Arctic Intermediate Water (AIW, θ ≤ 0 °C, σ_0 > 27.97, σ_0 ≤ 30.444) flows between 700 and 1500 m depth. Due to the small number of observations in this study, Deep Water (DW, σ_0 ≥ 30.444) included different water masses (Upper Polar Deep Water, UPDW; and Nordic Seas Deep Water, NDW) with potential temperatures between −0.89 and −0.66 °C, potential densities (σ_o) that ranged from 27.72 to 28.10 kg m^{-3}, and salinities between 34.91 and 34.93 (Rudels et al., 2005). Above the Greenland shelf, two main troughs in the seafloor determined the oceanic circulation and produced an anticyclonic surface circulation. Part of the water is carried by the EGC and returned through the WSC, flows northward along the Norske Trough to reach the 79NG glacier. It then continues into the Westwind Trough, which is the North-East Greenland Coastal Current (NEGCC) and presents a "C"-shaped distribution (Schaffer et al., 2017).

According with the results, three different zones were established based on the station bottom depth and the water masses. The Fram Strait region includes stations 1, 2, 3, 4, 5, 6, 8, 9, 16 and 25 whose depths exceed 790 m. This area was affected by the WSC current on the east and the EGC on the west, close to the shelf break, and the water masses found were: PSW, AAW, AIW, AW, RAW and DW. The shelf region comprises stations 10, 12 and 13 with bottom depths deeper than 170 m. The water masses identified here were the PSW and the AAW. Finally, the coastal region was influenced by the NEGCC, including stations 20, 22 and 24 (bottom depth > 178 m) and present PSW and AAW.

3.2. Cu-binding ligand distribution

For the determination of L_{Cu} in the seawater samples, two and one-ligand fitting was attempted; however, only one class of ligand was detected in each titration curve. The L_{Cu} concentrations in the study area ranged from 1.4 to 8.2 nM (Table 1), with the highest values present in the surface waters (<100 m depth, Fig. 2 and Supplementary material Table S3). The L_{Cu} concentrations showed a longitudinal trend with increasing values towards the Greenland coast (Figs. 1 and 2). Differences between stations located in Fram Strait, on the shelf and close to
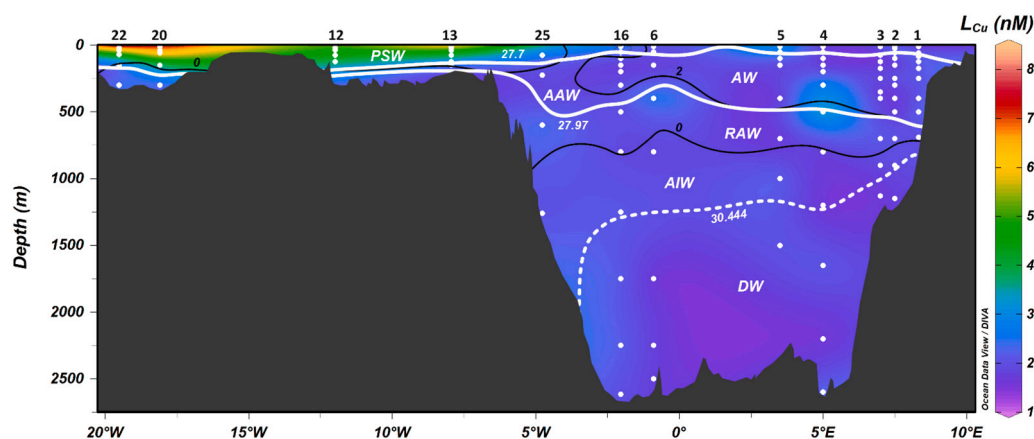
Fig. 2. Vertical distribution of Cu-binding ligands (L_{Cu} in nM) along a longitudinal transect from Svalbard to Greenland shelves. Potential temperature was depicted by black contour lines, potential density anomaly by white solid lines while dashed white line indicates the potential density anomaly of 30.444 estimated considering 500 dbar of pressure. Six water masses were identified: Polar Surface Water (PSW), Atlantic Water (AW), Recirculated Atlantic Water (RAW), Arctic Atlantic Water (AAW), Arctic Intermediate Water (AIW) and Deep Water (DW).

Table 1

Summary of results for dissolved copper binding ligand parameters calculated for the coast, shelf and Fram Strait regions. Minimum, maximum, mean with standard deviation ($\pm 1\sigma$) and median were reported.

Region	Stations		dCu (nM)	L_{Cu} (nM)	eL_{Cu} (nM)	log K_{Cu2+L}^{cond}	log α_{Cu2+L}	Cu^{2+} (fM)	Cu' (pM)	%CuL	L_{Cu}/dCu
Coast	20, 22, 24	Min	1.7	2.4	0.4	14.5	6.2	1.4	38.1	99.99	1.2
		Max	4.7	7.1	3.04	15.3	7.1	12.5	361.2	100	1.8
		Mean	3.5 ± 1.1	5.1 ± 1.9	1.60 ± 0.94	14.9 ± 0.3	6.6 ± 0.3	3.8 ± 2.8	111.1 ± 80.3	100.00 ± 0.0	1.4 ± 0.2
		Median	4.1	5.8	1.45	14.9	6.5	3.3	95.2	100	1.4
Shelf	10, 12, 13	Min	1.6	1.7	0.14	14.8	6.4	1.2	33.9	99.98	1.1
		Max	4.6	8.2	3.76	15.7	7.3	7.9	237.0	100	1.9
		Mean	3.0 ± 1.1	4.1 ± 1.7	1.05 ± 0.83	15.2 ± 0.3	6.8 ± 0.3	2.7 ± 1.8	78.7 ± 53.8	100.00 ± 0.0	1.3 ± 0.2
		Median	3.2	4.2	0.94	15.2	6.7	1.8	53.3	100	1.3
Fram Strait	1, 2, 3, 4, 5, 6, 8, 9, 16, 25	Min	1.2	1.4	0.03	14.3	5.8	0.1	3.9	99.96	1.0
		Max	5.2	6.0	1.84	16.3	7.7	21.1	633.8	100	2.2
		Mean	1.6 ± 0.5	2.2 ± 0.6	0.58 ± 0.34	15.5 ± 0.3	6.9 ± 0.3	1.7 ± 3.0	50.7 ± 87.6	100.00 ± 0.01	1.4 ± 0.2
		Median	1.5	2.0	0.57	15.6	6.9	0.8	23.8	100	1.4

the coast were observed, with significant (p-value<0.05) higher concentrations within the last two groups. On the shelf, L_{Cu} varied between 1.7 and 8.2 nM with higher concentrations at the surface with a local maximum (30 m depth) at St. 10 (8.2 nM). Coastal samples presented a L_{Cu} that range from 2.4 to 7.1 nM, with increasing concentrations observed at the surface waters. Fram Strait L_{Cu} varied between 1.4 and 6.0 nM.

In detail, the surface (<100 m depth) variability of L_{Cu} (1.4–8.2 nM) was higher than in deeper waters (L_{Cu} range 1.6–3.3 nM, at >100 m depth). In surface samples (Supplementary material Table S3) the observed L_{Cu} concentrations at the coast (mean value 6.4 ± 0.8 nM) and the shelf (mean value 5.2 ± 1.3 nM) presented significant differences (p-value<0.05, Supplementary material Table S1.b). However, below 100 m depth (Supplementary material Table S4), the L_{Cu} showed similar values with concentrations of 2.0 ± 0.4 nM in Fram Strait, 2.6 ± 0.7 nM on the Greenland shelf and 2.7 ± 0.6 nM near the coast, without significant differences between shelf and coastal stations (p-value>0.05, Supplementary material Table S1.c).

Station 9 (included in the Fram Strait group and with a bottom depth of 2544 m), located close to the shelf break, had L_{Cu} concentrations between 1.8 and 6.0 nM. This station showed a pronounced surface maximum and a minimum at depth, a distribution similar to the stations located on the shelf but differing from those located on the eastern Fram Strait.

In the study region, the dCu speciation was dominated by organic

complexation. The L_{Cu} concentrations were always in excess with respect to dCu (Tables 1 and S3), as indicated by the excess ligand concentration ($eL_{Cu} = L_{Cu} - dCu$; Tables 1 and S3). Notice that both L_{Cu} and eL_{Cu} depend strongly on the detection window applied. The eL_{Cu} ranged from 0.03 nM to 3.8 nM, with higher concentrations observed at the shelf and coastal stations. This indicates that the detected L_{Cu} were not fully saturated with dCu in solution. Coastal and shelf eL_{Cu} concentrations were significantly different to those from Fram Strait waters (p-value<0.05, Supplementary material Table S1a), but deeper waters (>100 m) appeared to be similar among the regions (p-value>0.05). The relationship between L_{Cu} and eL_{Cu} was linear (Fig. 3a) with a slight difference observed between surface samples <100 m, located close to the coast, on the shelf and at St. 9, and deeper samples (>100 m depth samples) from all the regions. The difference between surface and deep samples may indicate an extra source of L_{Cu} in surface waters that were not observed in the case of dCu. The distribution of L_{Cu} follows the pattern described for dCu (Supplementary material Fig. S2) with >99.9 % being organically complexed. Briefly, the concentration of dCu ranged from 1.2 to 5.2 nM (Table 1). Coastal and shelf stations presented a similar dCu concentration range (1.7–4.7 nM and 1.8–4.6 nM, respectively). The Fram Strait presented dCu concentrations between 1.2 and 2.5 nM, except St. 9 which showed a higher concentration range (1.5–5.2 nM) with a maximum at the surface. Dissolved Cu concentrations were strongly coupled to L_{Cu} (Fig. 3b) with a slightly higher correlation observed on the shelf ($R^2 = 0.83$, p-value<0.05) and near the
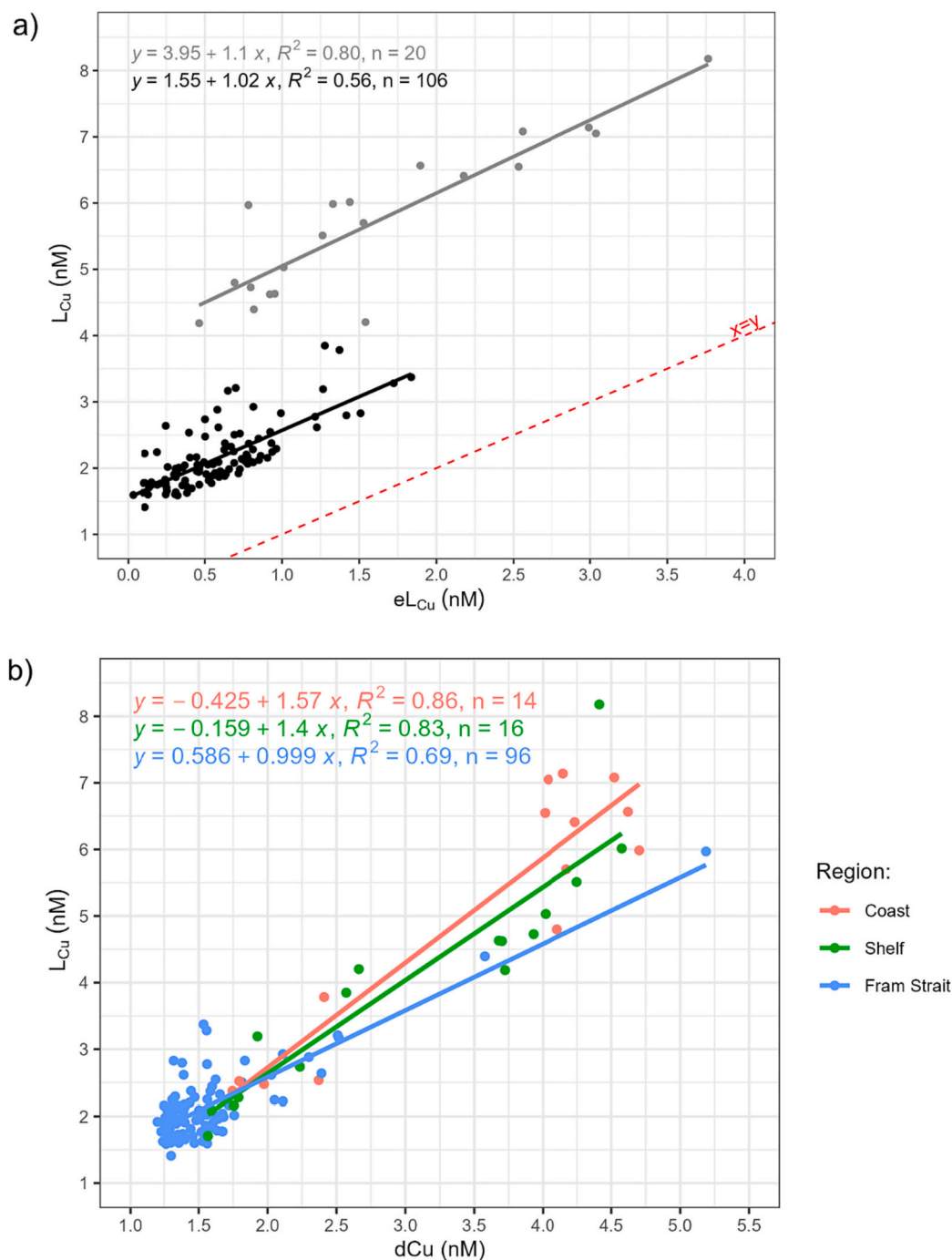
Fig. 3. a) Correlation between copper-binding ligand (L_{Cu}) and the excess ligand ($eL_{Cu} = L_{Cu} - dCu$) concentrations, both of them in nM. Surface samples (<100 m depth) located close to the coast (St. 20, 22 and 24), above the shelf (10, 12 and 13) and at St. 9 were represented in grey ($R^2 = 0.80$, p-value = $1.212e^{-7}$, n = 20). Black dots ($R^2 = 0.56$, p-value < $2.2e^{-16}$, n = 106) include samples deeper than 75 m from all the regions. The correlation between parameters was shown with solid lines. b) Correlation between copper-binding ligand (L_{Cu}) and dCu concentration (nM) with linear correlation estimated for coastal ($R^2 = 0.86$, p-value = $1.48e^{-6}$, n = 14), shelf ($R^2 = 0.83$, p-value = $1.08e^{-6}$, n = 16) and Fram Strait ($R^2 = 0.69$, p-value<$2.2e^{-16}$, n = 96) samples.

coast ($R^2 = 0.86$, p-value<0.05) than in Fram Strait ($R^2 = 0.69$, p-value<0.05). Samples with concentrations of L_{Cu} higher than 4 nM and dCu higher than 3.5 nM correspond to surface samples (<100 m depth) located close to the coast, on the shelf but also include St. 9.

Significant correlations ($R^2 = 0.84$, p-value<0.05) were observed between L_{Cu} concentration and salinity (Fig. 4). The region showed a salinity gradient between 29.87 and 35.14 where the lower salinities presented the highest L_{Cu} concentrations.

The relationship between the concentration of Cu-binding ligands and the class of ligands with the different water masses could help to identify potential sources. Table S5 and Fig. 5 present the concentration of L_{Cu} as a function of the water masses and location. In terms of water masses, significant differences were detected among stations located in the Fram Strait, the shelf and coastal waters. The highest L_{Cu} concentrations were found in PSW and the lowest in AW. In Fram Strait, the six water masses showed different L_{Cu} concentrations. The lowest L_{Cu} concentrations were observed in waters that come from the Atlantic Ocean (AW = 2.0 ± 0.3 nM) and deep waters (DW = 1.9 ± 0.2 nM). Fram Strait surface waters that contained waters from the Arctic Ocean showed higher L_{Cu} concentrations (PSW = 3.2 ± 1.1 nM and RAW = 2.3 ± 0.5
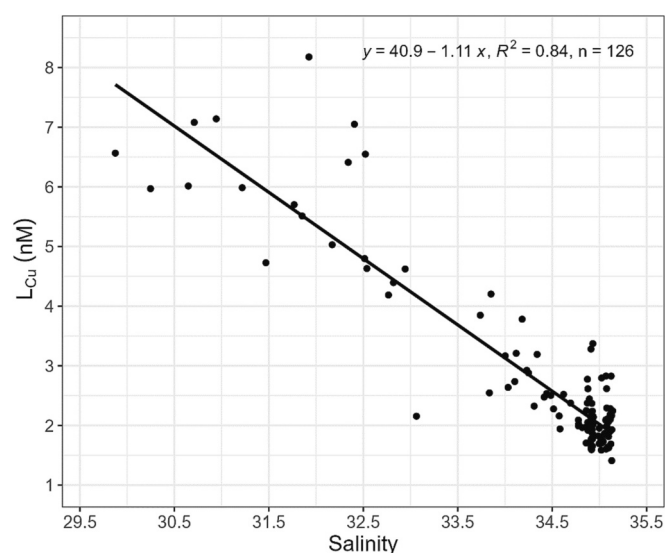
Fig. 4. Copper-binding ligand (L_{Cu}) concentration (nM) against salinity with a linear fitting applied on all samples collected along the study area ($R^2 = 0.84$, p-value $< 2.2e^{-16}$, n = 126). Samples with salinity lower than 33 differ significantly (p-value $= 4.418e^{-12}$) from samples with higher salinity.

nM). In the Fram Strait area, significant differences (p-value < 0.05), in terms of L_{Cu}, were observed between PSW and AW, AIW, RAW and DW. Shelf stations presented two water masses with L_{Cu} concentrations in PSW (4.7 ± 1.4 nM) higher than those observed in AAW (2.1 ± 0.3 nM). Cu-binding ligand differences between the water masses were significant (p-values < 0.05). Close to the coast, the mean L_{Cu} concentration observed on PSW (5.5 ± 1.7 nM) was higher than in AAW (2.5 ± 0.1 nM) with significant differences (p-values < 0.05). Water masses presented different concentrations of eL_{Cu}. The highest variabilities and concentrations were observed in PSW near the coast (mean $eL_{Cu} = 1.8 \pm 0.9$ nM) and on the shelf (mean $eL_{Cu} = 1.3 \pm 0.9$ nM), with the maximum eL_{Cu} value (3.8 nM) observed at St. 10 (30 m depth). Concentrations were also significantly different between AAW and PSW above the Greenland shelf (p-value < 0.05). The eastern Fram Strait showed the lowest variabilities (eL_{Cu} ranged from 0.03 to 1.8 nM) with minimum concentrations observed in DW and maximum in RAW. In this area, significant differences (p-value < 0.05) were observed between DW and AW, PSW and RAW.

3.3. Cu-binding ligand strengths

The conditional stability constants of L_{Cu}, which describes the strength of ligands, presented values between 14.2 and 16.3 (Table 1). The ligands detected in the entire region were classified as strong Cu-binding ligands, or L_1 class (Bruland et al., 2000; Buck and Bruland, 2005). The log K^{cond}_{Cu2+L} calculated is strongly conditioned by the detection window applied in each study. However, this current investigation has been conducted with the same detection windows as other oceanic publications, where both weak and strong ligands were detected (Abualhaija et al., 2015; Bundy et al., 2013; Hollister et al., 2021; Laglera and van den Berg, 2003; Whitby et al., 2018; Whitby and van den Berg, 2015; Wiwit et al., 2021). The values of log K^{cond}_{Cu2+L} observed along the three defined regions (Table 1 and Fig. 5) decrease towards the west (mean values Fram Strait $= 15.5 \pm 0.3$, shelf $= 15.2 \pm 0.3$ and coast $= 14.9 \pm 0.3$). In Fram Strait, log K^{cond}_{Cu2+L} was significantly different (p-value < 0.05, Supplementary material Table S1) than those observed on the shelf and in the coastal area. Most of this variability was observed in surface samples (Fram Strait $= 15.6 \pm 0.3$; shelf $= 15.2 \pm 0.3$; coast $= 14.8 \pm 0.3$; Supplementary material Table S3). Below 100 m depth, the log K^{cond}_{Cu2+L} presented lower variability with a mean value of $15.5 \pm$

0.4 (Fram Strait $= 15.5 \pm 0.3$.; shelf $= 15.0 \pm 0.2$; coast $= 15.2 \pm 0.2$; Supplementary material Table S4). No significant differences (p-value > 0.05) were observed between water masses inside each region (Supplementary material Table S2).

The reactivity of the natural Cu-binding ligands (α_{Cu2+L}) describes the capacity of dissolved ligands to be bound with Cu and is the product of the K^{cond}_{Cu2+L} and L_{Cu} (Gledhill and Gerringa, 2017). In the study area, log α_{Cu2+L} varied between 5.8 and 7.7 (Table 1, Fig. 5). Lower values were observed close to the coast (6.6 ± 0.3), intermediate values on the shelf (6.8 ± 0.3) and higher values in Fram Strait (6.9 ± 0.3). Significant differences (p-value < 0.05) were only observed between Fram Strait and the coast. Within each region, there were no statistical (p-value > 0.05) differences between water masses (Supplementary material Table S2).

3.4. Nutrient distribution and Cu-binding ligands relationship

The concentration of macronutrients ($NO_3^- + NO_2^-$, PO_4^{3-} and $Si(OH)_4$) in the study region were correlated with ligand concentrations (Fig. 6). Macronutrient concentrations were reported by Graeve et al. (2019) and described for the Fram Strait (Krisch et al., 2021, 2020; Tuerena et al., 2021). Briefly, differences in nutrient concentrations were observed between the eastern and western Fram Strait. Macronutrient concentrations increase at depth and the highest values were found in DW ($NO_3^- + NO_2^- = 12.32 \pm 2.05$ µM, $PO_4^{3-} = 0.84 \pm 0.18$ µM, $Si(OH)_4 = 9.46 \pm 2.15$ µM). Surface water masses showed different nutrient behaviours from west to east, the PSW presented relatively high concentrations of PO_4^{3-} (0.61 ± 0.17 µM) and $Si(OH)_4$ (4.74 ± 1.38 µM) but low $NO_3^- + NO_2^-$ (4.26 ± 3.42 µM) compared to AW ($NO_3^- + NO_2^- = 9.34 \pm 3.96$ µM, $PO_4^{3-} = 0.66 \pm 0.24$ µM, $Si(OH)_4 = 3.79 \pm 1.59$ µM). In Fram Strait, $NO_3^- + NO_2^-$ and PO_4^{3-} in PSW showed significant differences from the AIW and DW concentrations. However, $Si(OH)_4$ concentrations in Fram Strait presented significant differences between different water masses (Supplementary material Table S2). Close to the coast, the 79NG did not release significant amounts of nutrients.

The relationship between L_{Cu} and macronutrient concentrations was evaluated with linear fitting models (Fig. 6). Significant negative relationship was observed between both L_{Cu} and $NO_3^- + NO_2^-$ as well as between L_{Cu} and PO_4^{3-} levels. In the study region, no significant (p-value < 0.05) relationships were observed between Cu-binding ligand parameters (L_{Cu} and log K^{cond}_{Cu2+L}) and fluorescence.

4. Discussion

4.1. Copper complexation in the region

Most of the L_{Cu} concentrations observed in coastal and oceanic waters in the study region (1.4–8.2 nM) falls within the values typically reported in the open ocean (1–6 nM, Ruacho et al., 2022). However, the vertical distribution of L_{Cu} above the Greenland shelf contrasts with that obtained in the eastern Fram Strait, as well as the concentrations observed in oceanic and coastal waters, which exhibit increasing values with depth (Ruacho et al., 2022). The L_{Cu} concentrations observed in the eastern Fram Strait (1.2–5.2 nM) were similar to the values reported for strong ligands ($L_1 = 0.8$–5 nM) in the North Atlantic (2–2.5 µM SA, Gourain, 2020; Jacquot and Moffett, 2015) and the North Pacific Ocean (5 and 10 µM SA, Whitby et al., 2018; Wiwit et al., 2021; Wong et al., 2021). The surface maximum of L_{Cu} concentration reported for the Greenland shelf and coast (> 7 nM) exceeds surface values observed in the open ocean (~ 1 nM, Ruacho et al., 2022) and remains lower than concentrations detected in estuarine environments. In estuaries, a substantial quantity of L_1 (ranging from 1 to 33 nM) and L_2 (ranging from 14 to 300 nM) classes were detected (2.5 and 10 µM SA, Laglera and van den Berg, 2003; Muller and Batchelli, 2013). In other polar regions, such as the Canadian Arctic Archipelago and Baffin Bay, as well as Antarctic surface waters (Bundy et al., 2013; Nixon et al., 2019), L_{Cu} concentrations of up to 4 nM were observed, a level lower than those observed on
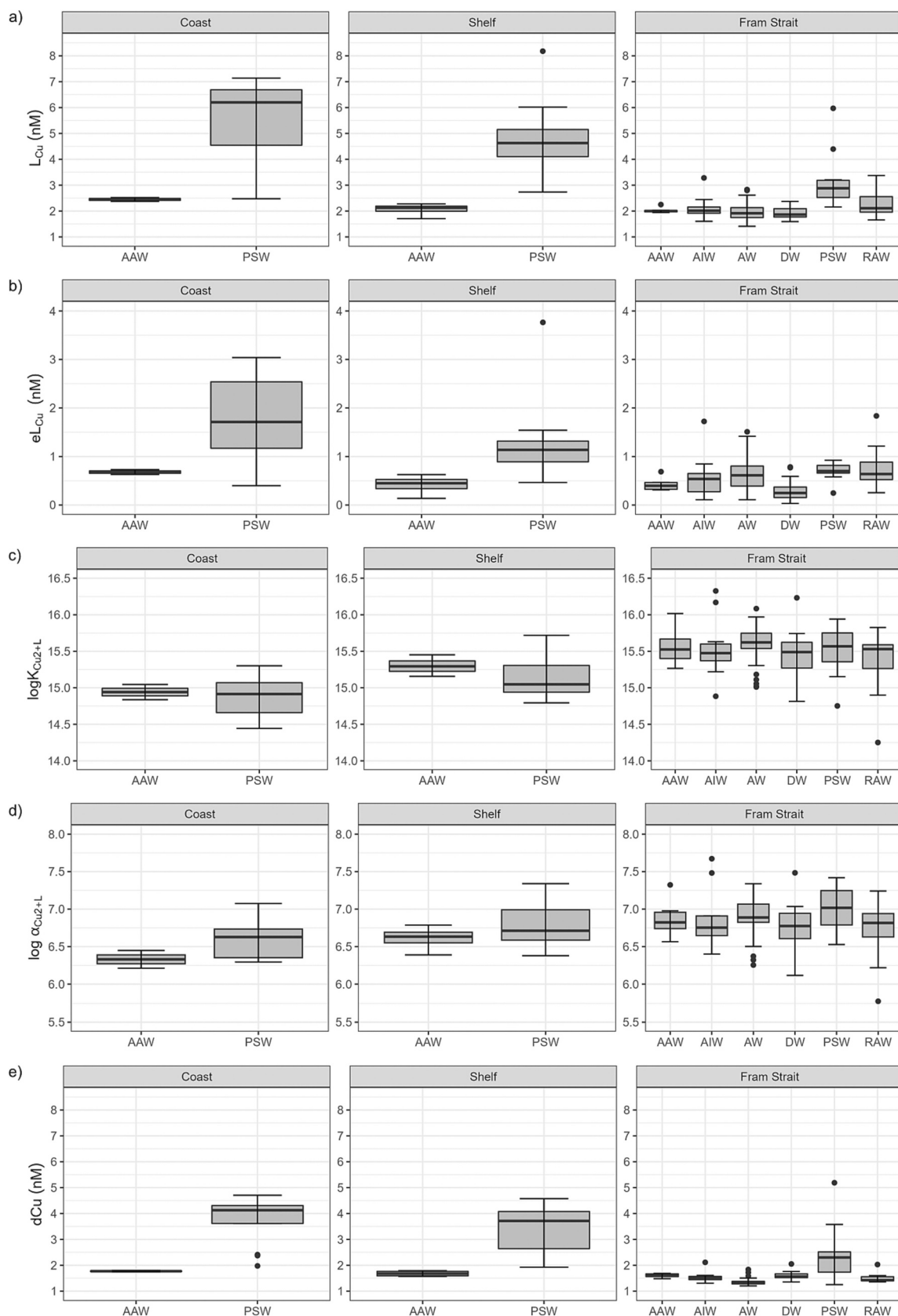
Fig. 5. Boxplots of the concentration of L_{Cu} (a), eL_{Cu} (b), log K_{Cu2+L}^{cond} (c), log f_{Cu2+L} (d), and dCu (e) from the station located on the Fram Strait, above the shelf and close to the coast categorized by water mass (Polar Surface Water, PSW, Atlantic Water, AW, Recirculated Atlantic Water, RAW, Arctic Atlantic Water, AAW, Arctic Intermediate Water, AIW, and Deep Water, DW). Circles indicate the outliers.
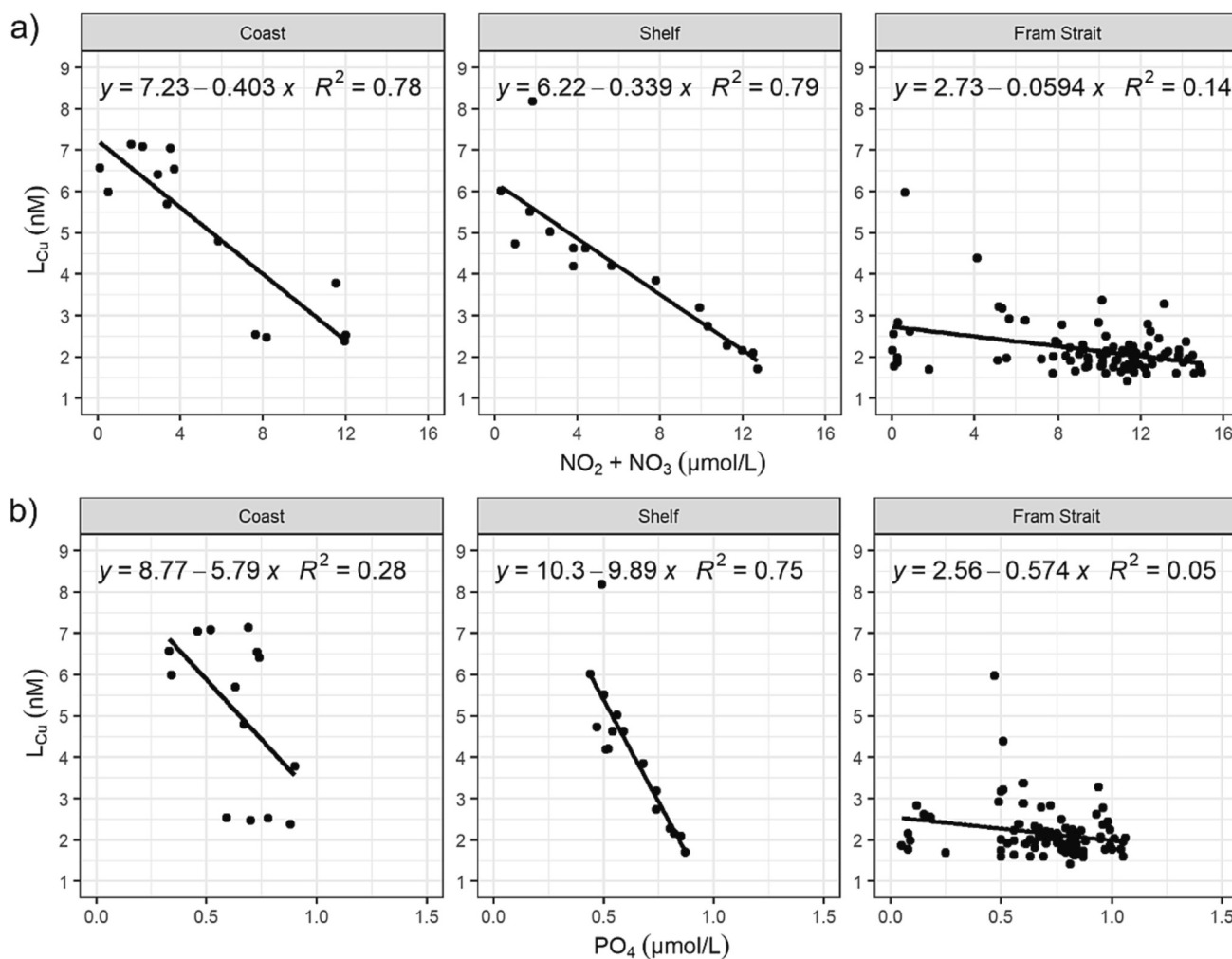
Fig. 6. Variability of Cu-binding ligand (L_{Cu} in nM) with respect to (a) nitrate and nitrite, and (b) phosphate concentrations (μmol/L). The number of samples (n) varies by region: 14 observations on the coast, 16 above the shelf and 95 in Fram Strait.

the Greenland shelf and coast (1.7–8.2 nM and 2.4–7.2 nM, respectively). However, similar to the Greenland shelf, the Canadian Arctic Archipelago and Baffin Bay also exhibited a surface maximum of L_{Cu} concentration associated with the biological production of L_{Cu} in surface waters. It is important to highlight that the method applied for ligand detection by Nixon et al. (2019) was immobilized Cu(II)-ion affinity chromatography and does not inform about the ligand binding strength.

The log K_{Cu2+L}^{cond} obtained in this study (14.3–16.3) corresponded to strong binding ligands (log $K_{Cu2+L}^{cond} > 13$, Buck and Bruland, 2005), exceeding the values between 12 and 14.8 reported for the North Atlantic Ocean (Gourain, 2020; Jacquot and Moffett, 2015). The North Pacific Ocean exhibited log K_{Cu2+L}^{cond} values for L_1 class ligands between 13.2 and 15.6 (Whitby et al., 2018; Wiwit et al., 2021; Wong et al., 2021), which were more similar to the results obtained in the study area. The log K_{Cu2+L}^{cond} values can be used to correlate the detected ligands with possible sources, which will be discussed in the next section.

It is important to remark that the results obtained using the voltammetric method are conditioned by the detection window applied. Concentrations of SA higher than 2.5 μM favour the detection of stronger ligands, while lower concentrations enable the detection of weaker compounds (Campos and van den Berg, 1994). The detection window applied in this study (10 μM SA) allowed the detection of strong ligands; however, in other regions, the same detection window enabled the measure of both strong and weak ligands (Laglera and van den Berg, 2003; Whitby et al., 2018; Wiwit et al., 2021). In natural waters, exists a continuum of ligands with varying strengths that may be detected or not

based on the experimental conditions. For this reason, the non-detection of weak ligands does not indicate their absence in the Arctic region. In addition, the use of the internal calibration method to establish the sensitivity is suitable for determining strong ligands, while it potentially reduces the detection of weak ligands (Pižeta et al., 2015). The presence and non-detection of weaker ligands (Campos and van den Berg, 1994), as well as the adsorption of organic compounds onto the Hg drop electrode (Kogut and Voelker, 2003), could impact the measurements of ligand concentration and binding strength. Furthermore, it is important to highlight that the log K_{Cu2+L}^{cond} obtained through voltammetry represents the average binding capacity of the ligand pool in each sample. Consequently, the presence of various natural ligand classes influences the determination of the conditional stability constant (Miller and Bruland, 1997).

4.2. Sources and sinks of Cu-binding ligands

Different mechanisms could explain the L_{Cu} concentrations and stability constants reported along the Fram Strait region, as well as the surface longitudinal variability reported.

4.2.1. Water mass circulation and influence from the TPD
The complex circulation patterns existing in Fram Strait (Laukert et al., 2017; Rudels et al., 2005; Schaffer et al., 2017) strongly influence the physico-chemical characteristics of waters, especially at the surface where most of the significant variabilities were measured.

The similarities in L_{Cu} concentration between the eastern Fram Strait and the North Atlantic can be attributed to the influence of the WSC, which brings Atlantic waters to the eastern part of the strait (Rudels et al., 2005). North Atlantic surface waters are characterized by low ligand concentrations (Gourain, 2020; Jacquot and Moffett, 2015; Ruacho et al., 2022) and relatively lower DOM levels compared to Arctic waters (Nguyen et al., 2022).

The high surface L_{Cu} concentrations reported for the shelf (~8 nM) and the maximum observed at St. 9 (~5 nM) could be related to the TPD, as suggested for Fe-binding ligands (Ardiningsih et al., 2020). The PSW observed above the Greenland shelf is related to the TPD and transported into the region by the EGC (Rudels et al., 2005). In the Arctic Ocean, the TPD carries high concentrations of DOM and trace metals from the Siberian shelves and rivers (Amon, 2003; Benner et al., 2005; Gerringa et al., 2021; Guéguen et al., 2007; Opsahl et al., 1999), including metal-binding ligands. To the extent of our knowledge, there is no information about Cu complexation from Siberian rivers. High concentrations of humic-like substances were observed inside the TPD (Gamrani et al., 2023; Gao and Guéguen, 2018) and correlated with Fe-binding ligands (Laglera et al., 2019; Slagter et al., 2019). This correlation was also detected in Fram Strait, where higher concentrations of Fe-binding ligands were observed above the Greenland shelf (Ardiningsih et al., 2020). Humic substances are not Fe-specific ligands and have been shown to complex Cu (Abualhaija et al., 2015), suggesting that a portion of the L_{Cu} pool may contain humic substances with riverine origin, as reported elsewhere (Hollister et al., 2021; Kogut and Voelker, 2001; Whitby et al., 2018; Whitby and van den Berg, 2015). Copper-binding humic substances detected in estuarine environments showed log K_{Cu2+L}^{cond} values between 14.9 and 15.9 (Muller and Batchelli, 2013) and do not explain the full range of log K_{Cu2+L}^{cond} (14.3–16.3) observed in the study area. The conditional stability constants observed in Fram Strait were also higher than the values of 12.1 reported for humic acids of different oceanic regions (Whitby and van den Berg, 2015). Other substances different from humics can be part of the L_{Cu} pool detected. For example, a portion of the riverine DOM transported towards the Fram Strait also contains thiol substances (Gao and Guéguen, 2018). Thiols have been identified as Cu-binding ligands in estuarine environments with variable conditional stability constants between 12 and 15 (Laglera and van den Berg, 2003; Whitby et al., 2017). In addition, laboratory studies with marine alga under copper stress conditions revealed conditional stability constants for Cu-binding ligands between 11.2 and 13 (Dupont et al., 2004; Leal et al., 1999; Walsh and Ahner, 2013). Then, thiols with the highest conditional stability constants could account for a part of the L_{Cu} pool detected in the study area. The input of riverine material into the study region can be supported by the relationship between L_{Cu} concentrations and salinity (Fig. 4). The correlation was observed exclusively within PSW, where samples with lower salinity exhibited the highest concentrations. Siberian rivers also discharge large quantities of dCu that were not scavenged on the shelf, enabling its transport to the Fram Strait by the TPD (Charette et al., 2020). This input of dCu is expected to be complexed by organic matter transported through the rivers, as observed in other coastal regions (Hoffmann et al., 2007; Muller and Batchelli, 2013; van den Berg et al., 1987; Williford et al., 2022). The strong complexation of dCu enables its transport within the Arctic Ocean and through the Fram Strait. The export of complexed Cu could be important in the regions that present Fe limitation, such as the south of Greenland and the Irminger Basin (Hopwood et al., 2018). As under Fe-limitation, some diatoms have higher Cu-requirements (Maldonado et al., 2006), this export of Cu-organically complexed from the Arctic Ocean towards the Nordic Seas and North Atlantic could support phytoplankton growth.

However, it must be noted that the coastal and shelf waters exhibited a lower dCu reactivity compared to the eastern Fram Strait, related to the longitudinal decrease of log K_{Cu2+L}^{cond} towards the west and the decline of log α_{Cu2+L} values (Table 1). In contrast to L_{Cu} and log K_{Cu2+L}^{cond}, log α_{Cu2+L} showed no significant variability between regions and water masses because the westward increase of L_{Cu} was countered by the decrease in log K_{Cu2+L}^{cond}.

4.2.2. Contributions from ice and glacial margins

The surface layer of Fram Strait also receive freshwater from sea-ice and the 79NG terminus. The highest concentrations of L_{Cu} and dCu were observed in surface waters above the shelf and close to the Greenland coast, an area that presented different sea-ice arrangements (data reported by König-Langlo, 2016). Sea-ice may act as a source of organic matter, trace metals, macronutrients, and sediments that were trapped in the ice when it was formed and released during melting (Evans and Nishioka, 2019; Thomas et al., 1995; Tovar-Sánchez et al., 2010). The sea-ice trace metal composition and size fractioning are a function of the location where the ice was formed, the age, the structure, and the processes that occur inside, such as biological degradation and reduction processes (Evans and Nishioka, 2019; Thomas et al., 1995; Tovar-Sánchez et al., 2010). A study carried out in the northwest of Svalbard revealed that the content of Cu in sea-ice (range from 30.4 to 67 nM) was much higher than that observed in seawater, with concentrations around 5 nM (Tovar-Sánchez et al., 2010). The first-year ice detected in the study region should contain lower nutrients and trace metal concentrations than multiyear Arctic ice (Tovar-Sánchez et al., 2010); however, part of the dCu detected in the western Fram Strait may come from the ice. On the other hand, the DOM observed in the northwest of Svalbard is more related to the biological production of protein-like substances (Zabłocka et al., 2020). Thus, part of the L_{Cu} and dCu observed in the western Fram Strait could be related to the ice. The biological production will be discussed in the following section.

Part of the observed coastal maximums of L_{Cu} and dCu could be related to the subglacial discharge of freshwater that may introduce nutrients, DOM, and trace metals into surface waters (Aciego et al., 2015; Cape et al., 2019; Hopwood et al., 2020; Krause et al., 2021). The release of DOM with glacial meltwater is 1–2 orders of magnitude lower than the inputs from Arctic rivers. However, it is likely more bioavailable due to its lower aromatic composition (Hopwood et al., 2020). The release of DOM might contribute to the L_{Cu} pool and may explain why, along the study area, the L_{Cu} concentrations increased towards the west while log K_{Cu2+L}^{cond} decreased. The longitudinal increase in L_{Cu} was stronger than dCu, an extra or more intense source of L_{Cu} compared to dCu is thus suggested (Fig. 3b). The contribution of dCu through subglacial discharge must be limited, as observed if we compare the concentration observed in coastal surface waters (maximum of 4.7 nM) with that reported for the central Arctic (~7 nM, Gerringa et al., 2021). However, studies made in different Greenlandic glaciers indicate that up to 2.5 nM of dCu could be released through glacial discharge (Krause et al., 2021).

The general decreasing relationship between L_{Cu} and $NO_3^- + NO_2^-$ and PO_4^{3-} (Fig. 6) observed on the shelf and coastal samples reinforce the hypothesis of coastal inputs of Cu-binding ligands. The highest L_{Cu} was related to the lowest $NO_3^- + NO_2^-$ concentrations at coastal and shelf samples and low PO_4^{3-} concentrations on the shelf (Fig. 6). The linear relationship observed concerning salinity (Supplementary material Fig. S3) in coastal ($R^2 = 0.86$) and shelf ($R^2 = 0.93$) waters for $NO_3^- + NO_2^-$ and on the shelf for PO_4^{3-} ($R^2 = 0.82$) indicate a low supply of these nutrients from Greenland glacial meltwater (Krisch et al., 2021, 2020; Meire et al., 2016; Tuerena et al., 2021) compared to the overwhelming supply of dCu and dCu-binding ligand from the central Arctic with the Transpolar Drift. This decrease in macronutrient concentrations with salinity could be related to a dilution of seawater properties due to the input of freshwater (Krause et al., 2021) that at the same time is adding Cu-binding ligands into the Fram Strait.

The extra supply of Cu-binding ligands in the coastal region could be exported to the shelf area by the NEGCC (Schaffer et al., 2017). This would explain the surface maximum of ligands observed at St. 10 (8.18 nM) and the corresponding log K_{Cu2+L}^{cond} (14.84).

4.2.3. Influence of biological activity

The phytoplankton community (mainly diatoms and bacteria) may contribute to Cu-binding ligands, as observed for the surface waters of the central Arctic and the Canadian Arctic Archipelago (Davis and Benner, 2005; Nixon et al., 2019; Williford et al., 2022). Phytoplankton blooms were described in Fram Strait (Lester et al., 2021) and could release L_{Cu} into the surface waters (Leal et al., 1999). This could contribute to the L_{Cu} pool detected in this study, as suggested for Fe-binding ligands (Ardiningsih et al., 2020). The algal sea-ice community produces high concentrations (26.2 ± 3.9 nM) of strong Cu-binding ligands (log K_{Cu2+L}^{cond} = 15.2 ± 0.3), as described by Bundy et al. (2013) for the Antarctic Peninsula. These values were higher than those reported above the Greenland shelf surface waters (L_{Cu} = 5.2 ± 1.3 nM; log K_{Cu2+L}^{cond} = 15.2 ± 0.3) but notice that sea-ice samples were not analysed. The characteristics of these Cu-binding ligands can be affected by melting, as the salinity is much lower than that of pore water. In addition, weak ligands such as exopolymer substances (EPS) may also present conditional stability constants lower than 10 (Ruacho et al., 2022). These substances were detected in Fram Strait sea-ice (Meiners et al., 2003) and described as Cu-binding ligands, exudates under Cu-stress conditions and extreme temperature and salinity (Krembs et al., 2002; Lin et al., 2020; Riedel et al., 2006). The EPS were suggested as part of the Fe-binding ligand pool in the Greenland shelf (Ardiningsih et al., 2020).

As mentioned above, log K_{Cu2+L}^{cond} showed decreasing values close to the Greenland coast, which produced lower log α_{Cu2+L} values (Table 1) and higher Cu^{2+} concentration (Table 1). In general terms, the Cu^{2+} concentration reported here (0.13–21.13 fM) does not exceed the toxicity limits (10 pM) established for different cyanobacteria, coccolithophores, and diatoms species (Brand et al., 1986; Sunda and Lewis, 1978). However, the concentration of Cu^{2+} reported could reduce phytoplankton growth and reproduction rates (Brand et al., 1986; Peers et al., 2005). Under Cu-limiting conditions, phytoplankton may actively release metal-binding ligands into the medium to acquire Cu (Walsh et al., 2015). Phytoplankton exudates may contain relatively weaker Cu-binding ligands, such as thiols with log K_{Cu2+L}^{cond} between 12 and 15 (Leal et al., 1999), which could contribute to the observed decrease in log K_{Cu2+L}^{cond}.

4.2.4. Sinks of Cu-binding ligands

In the study region, different mechanisms may reduce or transform Cu-binding ligands in seawater. As the concentration of Cu^{2+}, in terms of pCu^{2+} (pCu^{2+} = –log[Cu^{2+}]), was between 13.6 and 15.89, some phytoplankton species could experience Cu-limitation (Annett et al., 2008; Maldonado et al., 2006; Peers et al., 2005). Under Cu-deficient conditions, phytoplankton and diatoms fulfil their requirements through the release of strong and weak complexes (log K_{Cu2+L}^{cond} = 13.5–16, Semeniuk et al., 2015). Organic matter and metal-binding ligands can be transformed by microbial degradation (Paulsen et al., 2019) and photodegradation processes (Benner et al., 2005). The photodegradation of metal-binding ligands by solar irradiation in surface waters decreases the complexing capacity of Cu-binding ligands (Shank et al., 2006) and increases the Cu^{2+} bioavailability. The persistent sea-ice coverage in the Arctic limits the effect of solar irradiation, but ice-free surface waters may be subject to this degradation process and modify the ligand characteristics.

4.3. Future projections

The effects that climate change may have on trace metal speciation in the region are unknown. The higher Arctic riverine discharge of organic matter (Frey and McClelland, 2009; Stedmon et al., 2011) could increase the release of strong metal-binding ligands (Slagter et al., 2017) and trace metals (Guieu et al., 1996) into the surface waters of the Arctic Ocean. This could lead to an increase in L_{Cu} concentration on the Greenland shelf and coast and a higher export of Cu towards the Nordic

Seas and North Atlantic Ocean, as suggested for Fe (Ardiningsih et al., 2020). On the other hand, the thinning and retreat of 79NG ice tongue could produce higher meltwater discharge (Krisch et al., 2021) with stronger dissolved trace metal and DOM release close to the glacier terminus, which could alter the Cu-binding ligand concentrations. However, the reduction of sea-ice coverage may increase light penetration, the phytoplankton growth (Arrigo et al., 2008) as well as the photo-oxidation processes (Bélanger et al., 2006), with potential effects on Cu-binding ligand concentrations, utilisation, and nature. Finally, the intensification of the Atlantic water supply into the Fram Strait (Wang et al., 2020), alters the composition and productivity of the phytoplankton community (Ardyna and Arrigo, 2020) and consequently, the Cu-binding ligands.

According to the literature, an increase in seawater Cu^{2+} due to ocean acidification (Gledhill et al., 2015; Millero et al., 2009; Zuehlke and Kester, 1983), as well as the photooxidation processes (Shank et al., 2006). In addition, the decrease in pH is also expected to affect the Cu complexation (Gledhill et al., 2015). In the study region, the observed Cu^{2+} concentrations (0.13–21.13 fM) were low, possibly even limiting (Brand et al., 1986; Peers et al., 2005), and the Cu-binding ligand concentrations were high (1.4–8.2 nM). Accordingly, the toxic levels of Cu^{2+} for microorganisms are not easily achieved in the area under the projected changes in pH (Fransner et al., 2022). Finally, it is important to notice that the concentration of Cu along the Greenland coast could be influenced by mining activity in the region in the future (Søndergaard and Mosbech, 2022), which can be encouraged by the loss of ice coverage in terrestrial regions.

5. Conclusions

The current investigation presents the first data set of Cu-binding ligand concentrations (L_{Cu}) and the conditional stability constants (log K_{Cu2+L}^{cond}) for the Arctic region of Fram Strait, including the northeast Greenland shelf and coastal area. Three different zones have been identified along the region, from east to west designated as Fram Strait, the NE Greenland shelf and the Greenlandic coast. The L_{Cu} concentrations indicate a longitudinal trend with increasing values towards the west, especially in surface waters. Since the most elevated levels of L_{Cu} were detected near the 79NG glacier terminus, the coastal-to-ocean trend suggested that a portion of Cu-binding ligands of the Greenland shelf comes from the coastal sites and all the processes involved in the surrounding areas. The log K_{Cu2+L}^{cond} indicated the presence of strong binding ligands (L_1) and decreased towards the west. The organic matter degradation and/or bacterial remineralization, together with a minor contribution from coastal meltwater discharge, was suggested as the predominant processes that affect the L_{Cu} concentrations and characteristics in coastal waters. Shelf stations presented intermediate values between coastal and eastern Fram Strait samples due to the combined effect of coastal inputs and ligands exported from the central Arctic via the TPD. The Greenland shelf has distinct phenomena that determine the Cu-binding ligands characteristics, such as the interaction of the two currents (EGC and NEGCC), the presence of sea-ice and the biological activity (in sea-ice or phytoplankton blooms). The eastern Fram Strait presented the lowest L_{Cu} concentrations with results comparable to the North Atlantic Ocean.

The voltammetric technique does not provide information about the nature of organic ligands but allows us to determine the concentration and binding properties. The presence of excreted organic ligands by marine phytoplankton or sea-ice diatoms and degraded organic moieties was suggested to form the Cu-binding ligand pool, especially in coastal waters. However, it is to be expected that this pool of ligands in the region also contains humic substances with terrestrial origin. In addition, the presence of strong ligands keeps the Cu^{2+} at fM levels and allows the transport of Cu towards the Nordic Seas and North Atlantic Ocean.

In light of climate change and global warming, Arctic future

projections indicate a complex physical, chemical, and biological alteration of oceanic conditions. The biogeochemical responses are unclear and could have significant impacts on the biogeochemical cycle of trace metals, such as Cu. To understand how trace metals will behave, further investigation into the distribution, nature, and transformation of organic ligands in the Fram Strait and surrounding regions is necessary. This work represents a starting point for future studies to determine how climate change is going to affect copper speciation, and how the Fram Strait Atlantification may alter ligand concentration and copper toxicity.

CRediT authorship contribution statement

Declaration of competing interest

The authors declare that they have no known competing financial interests or personal relationships that could have appeared to influence the work reported in this paper.

Data availability

Data can be found online at https://doi.pangaea. de/10.1594/PANGAEA.959511.

Acknowledgements

Appendix A. Supplementary data

Supplementary data to this article can be found online at https://doi. org/10.1016/j.scitotenv.2023.168162.

References

Abualhaija, M.M., Whitby, H., van den Berg, C.M.G., 2015. Competition between copper and iron for humic ligands in estuarine waters. Mar. Chem. 172, 46–56. https://doi. org/10.1016/j.marchem.2015.03.010.

Aciego, S.M., Stevenson, E.I., Arendt, C.A., 2015. Climate versus geological controls on glacial meltwater micronutrient production in southern Greenland. Earth Planet. Sci. Lett. 424, 51–58. https://doi.org/10.1016/j.epsl.2015.05.017.

Amon, R.M.W., 2003. Dissolved organic carbon distribution and origin in the Nordic Seas: exchanges with the Arctic Ocean and the North Atlantic. J. Geophys. Res. 108, 3221. https://doi.org/10.1029/2002JC001594.

Annett, A.L., Lapi, S., Ruth, T.J., Maldonado, M.T., 2008. The effects of Cu and Fe availability on the growth and Cu:C ratios of marine diatoms. Limnol. Oceanogr. 53, 2451–2461. https://doi.org/10.4319/lo.2008.53.6.2451.

Ardiningsih, I., Krisch, S., Lodeiro, P., Reichart, G.J., Achterberg, E.P., Gledhill, M., Middag, R., Gerringa, L.J.A., 2020. Natural Fe-binding organic ligands in Fram Strait and over the northeast Greenland shelf. Mar. Chem. 224, 103815 https://doi.org/10.1016/j.marchem.2020.103815.

Ardyna, M., Arrigo, K.R., 2020. Phytoplankton dynamics in a changing Arctic Ocean. Nat. Clim. Chang. 10, 892–903. https://doi.org/10.1038/s41558-020-0905-y.

Arrigo, K.R., van Dijken, G., Pabi, S., 2008. Impact of a shrinking Arctic ice cover on marine primary production. Geophys. Res. Lett. 35, L19603 https://doi.org/10.1029/2008GL035028.

Bélanger, S., Xie, H., Krotkov, N., Larouche, P., Vincent, W.F., Babin, M., 2006. Photomineralization of terrigenous dissolved organic matter in Arctic coastal waters from 1979 to 2003: interannual variability and implications for climate change. Glob. Biogeochem. Cycles 20, n/a–n/a. https://doi.org/10.1029/2006GB002708.

Benner, R., Louchouarn, P., Amon, R.M.W., 2005. Terrigenous dissolved organic matter in the Arctic Ocean and its transport to surface and deep waters of the North Atlantic. Glob. Biogeochem. Cycles 19. https://doi.org/10.1029/2004GB002398.

Brand, L.E., Sunda, W.G., Guillard, R.R.L., 1986. Reduction of marine phytoplankton reproduction rates by copper and cadmium. J. Exp. Mar. Biol. Ecol. 96, 225–250. https://doi.org/10.1016/0022-0981(86)90205-4.

Bruland, K.W., Rue, E.L., Donat, J.R., Skrabal, S.A., Moffett, J.W., 2000. Intercomparison of voltammetric techniques to determine the chemical speciation of dissolved copper in a coastal seawater sample. Anal. Chim. Acta 405, 99–113. https://doi.org/10.1016/S0003-2670(99)00675-3.

Buck, K.N., Bruland, K.W., 2005. Copper speciation in San Francisco Bay: a novel approach using multiple analytical windows. Mar. Chem. 96, 185–198. https://doi.org/10.1016/j.marchem.2005.01.001.

Bundy, R.M., Barbeau, K.A., Buck, K.N., 2013. Sources of strong copper-binding ligands in Antarctic Peninsula surface waters. Deep-Sea Res. II Top. Stud. Oceanogr. 90, 134–146. https://doi.org/10.1016/j.dsr2.2012.07.023.

Cai, W.J., Chen, L., Chen, B., Gao, Z., Lee, S.H., Chen, J., Pierrot, D., Sullivan, K., Wang, Y., Hu, X., Huang, W.J., Zhang, Y., Xu, S., Murata, A., Grebmeier, J.M., Jones, E.P., Zhang, H., 2010. Decrease in the CO$_2$ uptake capacity in an ice-free Arctic Ocean basin. Science 1979 (329), 556–559. https://doi.org/10.1126/science.1189338.

Campos, M.L.A.M., van den Berg, C.M.G., 1994. Determination of copper complexation in sea water by cathodic stripping voltammetry and ligand competition with salicylaldoxime. Anal. Chim. Acta 284, 481–496.

Cape, M.R., Straneo, F., Beaird, N., Bundy, R.M., Charette, M.A., 2019. Nutrient release to oceans from buoyancy-driven upwelling at Greenland tidewater glaciers. Nat. Geosci. 12, 34–39. https://doi.org/10.1038/s41561-018-0268-4.

Charette, M.A., Kipp, L.E., Jensen, L.T., Dabrowski, J.S., Whitmore, L.M., Fitzsimmons, J. N., Williford, T., Ulfsbo, A., Jones, E., Bundy, R.M., Vivancos, S.M., Pahnke, K., John, S.G., Xiang, Y., Hatta, M., Petrova, M.v, Heimbürger-Boavida, L., Bauch, D., Newton, R., Pasqualini, A., Agather, A.M., Amon, R.M.W., Anderson, R.F., Andersson, P.S., Benner, R., Bowman, K.L., Edwards, R.L., Gdaniec, S., Gerringa, L.J. A., González, A.G., Granskog, M., Haley, B., Hammerschmidt, C.R., Hansell, D.A., Henderson, P.B., Kadko, D.C., Kaiser, K., Laan, P., Lam, P.J., Lamborg, C.H., Levier, M., Li, X., Margolin, A.R., Measures, C., Middag, R., Millero, F.J., Moore, W. S., Paffrath, R., Planquette, H., Rabe, B., Reader, H., Rember, R., Rijkenberg, M.J.A., Roy-Barman, M., Rutgers van der Loeff, M., Saito, M., Schauer, U., Schlosser, P., Sherrell, R.M., Shiller, A.M., Slagter, H., Sonke, J.E., Stedmon, C., Woosley, R.J., Valk, O., Ooijen, J., Zhang, R., 2020. The transpolar drift as a source of riverine and shelf-derived trace elements to the central Arctic Ocean. J. Geophys. Res. Oceans 125, 1–34. https://doi.org/10.1029/2019JC015920.

Choi, D.W., Zea, C.J., Do, Y.S., Semrau, J.D., Antholine, W.E., Hargrove, M.S., Pohl, N.L., Boyd, E.S., Geesey, G.G., Hartsel, S.C., Shafe, P.H., McEllistrem, M.T., Kisting, C.J., Campbell, C., Rao, V., de la Mora, A.M., DiSpirito, A.A., 2006. Spectral, kinetic, and thermodynamic properties of Cu(I) and Cu(II) binding by methanobactin from *Methylosinus trichosporium* OB3b. Biochemistry 45, 1442–1453. https://doi.org/10.1021/bi051815t.

Conover, W.J., Iman, R.L., 1979. On multiple-comparisons procedures. In: Los Alamos Sci. Lab. Tech. Rep. LA-7677-MS 1, p. 14.

Cutter, G., Andersson, P., Codispoti, L., Croot, P., Francois, R., Lohan, M., Obata, H., Rutgers van der Loeff, M., 2010. Sampling and Sample-handling Protocols for GEOTRACES Cruises.

Davis, J., Benner, R., 2005. Seasonal trends in the abundance, composition and bioavailability of particulate and dissolved organic matter in the Chukchi/Beaufort Seas and western Canada Basin. Deep-Sea Res. II Top. Stud. Oceanogr. 52, 3396–3410. https://doi.org/10.1016/j.dsr2.2005.09.006.

Dupont, C.L., Nelson, R.K., Moffett, J.W., Ahner, B.A., 2004. Novel copper-binding and nitrogen-rich thiols produced and exuded by Emiliania huxleyi. Limnol. Oceanogr. 49, 1754–1762. https://doi.org/10.4319/lo.2004.49.5.1754.

Evans, L.K., Nishioka, J., 2019. Accumulation processes of trace metals into Arctic sea ice: distribution of Fe, Mn and Cd associated with ice structure. Mar. Chem. 209, 36–47. https://doi.org/10.1016/j.marchem.2018.11.011.

Feng, D., Gleason, C.J., Lin, P., Yang, X., Pan, M., Ishitsuka, Y., 2021. Recent changes to Arctic river discharge. Nat. Commun. 12, 6917. https://doi.org/10.1038/s41467-021-27228-1.

Fransner, F., Fröb, F., Tjiputra, J., Goris, N., Lauvset, S.K., Skjelvan, I., Jeansson, E., Omar, A., Chierici, M., Jones, E., Fransson, A., Ólafsdóttir, S.R., Johannessen, T., Olsen, A., 2022. Acidification of the Nordic Seas. Biogeosciences 19, 979–1012. https://doi.org/10.5194/bg-19-979-2022.

Frey, K.E., McClelland, J.W., 2009. Impacts of permafrost degradation on arctic river biogeochemistry. Hydrol. Process. 23, 169–182. https://doi.org/10.1002/hyp.7196.

Gamrani, M., Eert, J., Williams, W.J., Guéguen, C., 2023. A river of terrestrial dissolved organic matter in the upper waters of the central Arctic Ocean. Deep-Sea Res. I Oceanogr. Res. Pap. 196, 104016 https://doi.org/10.1016/j.dsr.2023.104016.

Gao, Z., Guéguen, C., 2018. Distribution of thiol, humic substances and colored dissolved organic matter during the 2015 Canadian Arctic GEOTRACES cruises. Mar. Chem. 203, 1–9. https://doi.org/10.1016/j.marchem.2018.04.001.

Gerringa, L., Rijkenberg, M.J.A., Slagter, H.A., Laan, P., Paffrath, R., Bauch, D., Rutgers van der Loeff, M., Middag, R., 2021. Dissolved Cd, Co, Cu, Fe, Mn, Ni, and Zn in the Arctic Ocean. J. Geophys. Res. Oceans 126. https://doi.org/10.1029/2021JC017323.

Gledhill, M., Gerringa, L.J.A., 2017. The effect of metal concentration on the parameters derived from complexometric titrations of trace elements in seawater—a model study. Front. Mar. Sci. 4, 1–15. https://doi.org/10.3389/fmars.2017.00254.

Gledhill, M., Achterberg, E.P., Li, K., Mohamed, K.N., Rijkenberg, M.J.A., 2015. Influence of ocean acidification on the complexation of iron and copper by organic ligands in estuarine waters. Mar. Chem. 177, 421–433. https://doi.org/10.1016/j.marchem.2015.03.016.

Goñi, M.A., O'Connor, A.E., Kuzyk, Z.Z., Yunker, M.B., Gobeil, C., Macdonald, R.W., 2013. Distribution and sources of organic matter in surface marine sediments across the North American Arctic margin. J. Geophys. Res. Oceans 118, 4017–4035. https://doi.org/10.1002/jgrc.20286.

Gordienko, P.A., Laktionov, A.F., 1969. Circulation and physics of the Arctic Basin waters. In: Gordon, A.L., Baker, F.W.G. (Eds.), Oceanography. Elsevier, pp. 94–112.

Gourain, C.G., 2020. Copper Biogeochemical Cycle and the Organic Complexation of Dissolved Copper in the North Atlantic. University of Liverpool. https://doi.org/10.17638/03083646.

Graeve, M., Ludwichowski, K.-U., Krisch, S., 2019. Inorganic Nutrients Measured on Water Bottle Samples From Ultra Clean CTD/Water Sampler-system During POLARSTERN Cruise PS100 (ARK-XXX/2), Version 2. https://doi.org/10.1594/PANGAEA.905347.

Granskog, M.A., Stedmon, C.A., Dodd, P.A., Amon, R.M.W., Pavlov, A.K., de Steur, L., Hansen, E., 2012. Characteristics of colored dissolved organic matter (CDOM) in the Arctic outflow in the Fram Strait: assessing the changes and fate of terrigenous CDOM in the Arctic Ocean. J. Geophys. Res. Oceans 117. https://doi.org/10.1029/2012JC008075 (n/a-n/a).

Guéguen, C., Guo, L., Yamamoto-Kawai, M., Tanaka, N., 2007. Colored dissolved organic matter dynamics across the shelf-basin interface in the western Arctic Ocean. J. Geophys. Res. 112, C05038 https://doi.org/10.1029/2006JC003584.

Guieu, C., Huang, W.W., Martin, J.-M., Yong, Y.Y., 1996. Outflow of trace metals into the Laptev Sea by the Lena River. Mar. Chem. 53, 255–267. https://doi.org/10.1016/0304-4203(95)00093-3.

Hoffmann, S.R., Shafer, M.M., Armstrong, D.E., 2007. Strong colloidal and dissolved organic ligands binding copper and zinc in rivers. Environ. Sci. Technol. 41, 6996–7002. https://doi.org/10.1021/es070958v.

Hollister, A.P., Whitby, H., Seidel, M., Lodeiro, P., Gledhill, M., Koschinsky, A., 2021. Dissolved concentrations and organic speciation of copper in the Amazon River estuary and mixing plume. Mar. Chem. 234, 104005 https://doi.org/10.1016/j.marchem.2021.104005.

Hopwood, M.J., Carroll, D., Browning, T.J., Meire, L., Mortensen, J., Krisch, S., Achterberg, E.P., 2018. Non-linear response of summertime marine productivity to increased meltwater discharge around Greenland. Nat. Commun. 9, 3256. https://doi.org/10.1038/s41467-018-05488-8.

Hopwood, M.J., Carroll, D., Dunse, T., Hodson, A., Holding, J.M., Iriarte, J.L., Ribeiro, S., Achterberg, E.P., Cantoni, C., Carlson, D.F., Chierici, M., Clarke, J.S., Cozzi, S., Fransson, A., Juul-Pedersen, T., Winding, M.H.S., Meire, L., 2020. Review article: how does glacier discharge affect marine biogeochemistry and primary production in the Arctic? Cryosphere 14, 1347–1383. https://doi.org/10.5194/tc-14-1347-2020.

IPCC, 2022. Global Warming of 1.5°C. Cambridge University Press. https://doi.org/10.1017/9781009157940.

Jacquot, J.E., Moffett, J.W., 2015. Copper distribution and speciation across the International GEOTRACES Section GA03. Deep-Sea Res. II Top. Stud. Oceanogr. 116, 187–207. https://doi.org/10.1016/j.dsr2.2014.11.013.

Kanzow, T., 2016. The Expedition PS100 of the Research Vessel POLARSTERN to the Fram Strait in 2016. https://doi.org/10.2312/BzPM_0705_2017.

Kogut, M.B., Voelker, B.M., 2001. Strong copper-binding behavior of terrestrial humic substances in seawater. Environ. Sci. Technol. 35, 1149–1156. https://doi.org/10.1021/es0014584.

Kogut, M.B., Voelker, B.M., 2003. Kinetically inert Cu in coastal waters. Environ. Sci. Technol. 37, 509–518. https://doi.org/10.1021/es020723d.

König-Langlo, G., 2016. Meteorological Observations During POLARSTERN Cruise PS100 (ARK-XXX/2). https://doi.org/10.1594/PANGAEA.868103.

Kramer, C.J.M., 1986. Apparent copper complexation capacity and conditional stability constants in North Atlantic waters. Mar. Chem. 18, 335–349. https://doi.org/10.1016/0304-4203(86)90016-2.

Krause, J., Hopwood, M.J., Höfer, J., Krisch, S., Achterberg, E.P., Alarcón, E., Carroll, D., González, H.E., Juul-Pedersen, T., Liu, T., Lodeiro, P., Meire, L., Rosing, M.T., 2021. Trace element (Fe, Co, Ni and Cu) dynamics across the salinity gradient in Arctic and Antarctic glacier fjords. Front Earth Sci. (Lausanne) 9. https://doi.org/10.3389/feart.2021.725279.

Krembs, C., Eicken, H., Junge, K., Deming, J.W., 2002. High concentrations of exopolymeric substances in Arctic winter sea ice: implications for the polar ocean carbon cycle and cryoprotection of diatoms. Deep-Sea Res. I Oceanogr. Res. Pap. 49, 2163–2181. https://doi.org/10.1016/S0967-0637(02)00122-X.

Krisch, S., Browning, T.J., Graeve, M., Ludwichowski, K.U., Lodeiro, P., Hopwood, M.J., Roig, S., Yong, J.C., Kanzow, T., Achterberg, E.P., 2020. The influence of Arctic Fe and Atlantic fixed N on summertime primary production in Fram Strait, North Greenland Sea. Sci. Rep. 10, 15230. https://doi.org/10.1038/s41598-020-72100-9.

Krisch, S., Hopwood, M.J., Schaffer, J., Al-Hashem, A., Höfer, J., Rutgers van der Loeff, M.M., Conway, T.M., Summers, B.A., Lodeiro, P., Ardiningsih, I., Steffens, T., Achterberg, E.P., 2021. The 79°N glacier cavity modulates subglacial iron export to the NE Greenland Shelf. Nat. Commun. 12, 3030. https://doi.org/10.1038/s41467-021-23093-0.

Krisch, S., Hopwood, M.J., Roig, S., Gerringa, L.J.A., Middag, R., Rutgers van der Loeff, M.M., Petrova, M.V., Lodeiro, P., Colombo, M., Cullen, J.T., Jackson, S.L., Heimbürger-Boavida, L., Achterberg, E.P., 2022. Arctic–Atlantic exchange of the dissolved micronutrients iron, manganese, cobalt, nickel, copper and zinc with a focus on Fram Strait. Glob. Biogeochem. Cycles 36. https://doi.org/10.1029/2021GB007191.

Krumpen, T., Belter, H.J., Boetius, A., Damm, E., Haas, C., Hendricks, S., Nicolaus, M., Nöthig, E.M., Paul, S., Peeken, I., Ricker, R., Stein, R., 2019. Arctic warming interrupts the Transpolar Drift and affects long-range transport of sea ice and ice-rafted matter. Sci. Rep. 9, 5459. https://doi.org/10.1038/s41598-019-41456-y.

Kruskal, W.H., Wallis, W.A., 1952. Use of ranks in one-criterion variance analysis. J. Am. Stat. Assoc. 47, 583–621.

Laglera, L.M., van den Berg, C.M.G., 2003. Copper complexation by thiol compounds in estuarine waters. Mar. Chem. 82, 71–89. https://doi.org/10.1016/S0304-4203(03)00053-7.

Laglera, L.M., Sukekava, C., Slagter, H.A., Downes, J., Aparicio-Gonzalez, A., Gerringa, L. J.A., 2019. First quantification of the controlling role of humic substances in the transport of iron across the surface of the Arctic Ocean. Environ. Sci. Technol. 53, 13136–13145. https://doi.org/10.1021/acs.est.9b04240.

Laukert, G., Frank, M., Bauch, D., Hathorne, E.C., Rabe, B., von Appen, W.J., Wegner, C., Zieringer, M., Kassens, H., 2017. Ocean circulation and freshwater pathways in the Arctic Mediterranean based on a combined Nd isotope, REE and oxygen isotope section across Fram Strait. Geochim. Cosmochim. Acta 202, 285–309. https://doi.org/10.1016/j.gca.2016.12.028.

Leal, M.F.C., Vasconcelos, M.T.S.D., van den Berg, C.M.G., 1999. Copper-induced release of complexing ligands similar to thiols by Emiliania huxleyi in seawater cultures. Limnol. Oceanogr. 44, 1750–1762. https://doi.org/10.4319/lo.1999.44.7.1750.

Lester, C.W., Wagner, T.J.W., McNamara, D.E., Cape, M.R., 2021. The influence of meltwater on phytoplankton blooms near the sea-ice edge. Geophys. Res. Lett. 48 https://doi.org/10.1029/2020GL091758.

Lin, H., Wang, C., Zhao, H., Chen, G., Chen, X., 2020. A subcellular level study of copper speciation reveals the synergistic mechanism of microbial cells and EPS involved in copper binding in bacterial biofilms. Environ. Pollut. 263, 114485 https://doi.org/10.1016/j.envpol.2020.114485.

Lombardi, A.T., Hidalgo, T.M.R., Vieira, A.A.H., 2005. Copper complexing properties of dissolved organic materials exuded by the freshwater microalgae Scenedesmus acuminatus (Chlorophyceae). Chemosphere 60, 453–459. https://doi.org/10.1016/j.chemosphere.2004.12.071.

Maldonado, M.T., Allen, A.E., Chong, J.S., Lin, K., Leus, D., Karpenko, N., Harris, S.L., 2006. Copper-dependent iron transport in coastal and oceanic diatoms. Limnol. Oceanogr. 51, 1729–1743. https://doi.org/10.4319/lo.2006.51.4.1729.

Meiners, K., Gradinger, R., Fehling, J., Civitarese, G., Spindler, M., 2003. Vertical distribution of exopolymer particles in sea ice of the Fram Strait (Arctic) during autumn. Mar. Ecol. Prog. Ser. 248, 1–13. https://doi.org/10.3354/meps248001.

Meire, L., Meire, P., Struyf, E., Krawczyk, D.W., Arendt, K.E., Yde, J.C., Juul Pedersen, T., Hopwood, M.J., Rysgaard, S., Meysman, F.J.R., 2016. High export of dissolved silica from the Greenland Ice Sheet. Geophys. Res. Lett. 43, 9173–9182. https://doi.org/10.1002/2016GL070191.

Miller, L.A., Bruland, K.W., 1997. Competitive equilibration techniques for determining transition metal speciation in natural waters: evaluation using model data. Anal. Chim. Acta 343, 161–181. https://doi.org/10.1016/S0003-2670(96)00565-X.

Millero, F.J., Woosley, R., Ditrolio, B., Waters, J., 2009. Effect of ocean acidification on the speciation of metals in seawater, 22, 72–85. https://doi.org/10.2307/24861025.

Moffett, J.W., Dupont, C., 2007. Cu complexation by organic ligands in the sub-arctic NW Pacific and Bering Sea. Deep Sea Res. I 54, 586–595. https://doi.org/10.1016/j.dsr.2006.12.013.

Muller, F.L.L., Batchelli, S., 2013. Copper binding by terrestrial versus marine organic ligands in the coastal plume of River Thurso, North Scotland. Estuar. Coast. Shelf Sci. 133, 137–146. https://doi.org/10.1016/j.ecss.2013.08.024.

Nguyen, H.T., Lee, Y.M., Hong, J.K., Hong, S., Chen, M., Hur, J., 2022. Climate warming-driven changes in the flux of dissolved organic matter and its effects on bacterial communities in the Arctic Ocean: a review. Front. Mar. Sci. 9 https://doi.org/10.3389/fmars.2022.968583.

Nixon, R.L., Jackson, S.L., Cullen, J.T., Ross, A.R.S., 2019. Distribution of copper-complexing ligands in Canadian Arctic waters as determined by immobilized copper (II)-ion affinity chromatography. Mar. Chem., 103673 https://doi.org/10.1016/j.marchem.2019.103673.

Omanović, D., Garnier, C., Pižeta, I., 2015. ProMCC: an all-in-one tool for trace metal complexation studies. Mar. Chem. 173, 25–39. https://doi.org/10.1016/j.marchem.2014.10.011.

Opsahl, S., Benner, R., Amon, R.M.W., 1999. Major flux of terrigenous dissolved organic matter through the Arctic Ocean. Limnol. Oceanogr. 44, 2017–2023. https://doi.org/10.4319/lo.1999.44.8.2017.

Paulsen, M.L., Müller, O., Larsen, A., Møller, E.F., Middelboe, M., Sejr, M.K., Stedmon, C., 2019. Biological transformation of Arctic dissolved organic matter in a NE Greenland fjord. Limnol. Oceanogr. 64, 1014–1033. https://doi.org/10.1002/lno.11091.

Peers, G., Quesnel, S.A., Price, N.M., 2005. Copper requirements for iron acquisition and growth of coastal and oceanic diatoms. Limnol. Oceanogr. 50, 1149–1158. https://doi.org/10.4319/lo.2005.50.4.1149.

Peterson, B.J., Holmes, R.M., McClelland, J.W., Vörösmarty, C.J., Lammers, R.B., Shiklomanov, A.I., Shiklomanov, I.A., Rahmstorf, S., 2002. Increasing river discharge to the Arctic Ocean. Science 1979 (298), 2171–2173. https://doi.org/10.1126/science.1077445.

Pfirman, S.L., Kögeler, J.W., Rigor, I., 1997. Potential for rapid transport of contaminants from the Kara Sea. Sci. Total Environ. 202, 111–122. https://doi.org/10.1016/S0048-9697(97)00108-3.

Pižeta, I., Sander, S.G., Hudson, R.J.M., Omanović, D., Baars, O., Barbeau, K.A., Buck, K.N., Bundy, R.M., Carrasco, G., Croot, P.L., Garnier, C., Gerringa, L.J.A., Gledhill, M., Hirose, K., Kondo, Y., Laglera, L.M., Nuester, J., Rijkenberg, M.J.A., Takeda, S., Twining, B.S., Wells, M., 2015. Interpretation of complexometric titration data: an intercomparison of methods for estimating models of trace metal complexation by natural organic ligands. Mar. Chem. 173, 3–24. https://doi.org/10.1016/j.marchem.2015.03.006.

Rapp, I., Schlosser, C., Rusiecka, D., Gledhill, M., Achterberg, E.P., 2017. Automated preconcentration of Fe, Zn, Cu, Ni, Cd, Pb, Co, and Mn in seawater with analysis using high-resolution sector field inductively-coupled plasma mass spectrometry. Anal. Chim. Acta 976, 1–13. https://doi.org/10.1016/j.aca.2017.05.008.

Riedel, A., Michel, C., Gosselin, M., 2006. Seasonal study of sea-ice exopolymeric substances on the Mackenzie shelf: implications for transport of sea-ice bacteria and algae. Aquat. Microb. Ecol. 45, 195–206.

Rignot, E., Mouginot, J., 2012. Ice flow in Greenland for the International Polar Year 2008-2009. Geophys. Res. Lett. 39 https://doi.org/10.1029/2012GL051634 (n/a-n/a).

Ruacho, A., Richon, C., Whitby, H., Bundy, R.M., 2022. Sources, sinks, and cycling of dissolved organic copper binding ligands in the ocean. Commun. Earth Environ. 3, 263. https://doi.org/10.1038/s43247-022-00597-1.

Rudels, B., 2019. Arctic Ocean circulation. In: Encyclopedia of Ocean Sciences. Elsevier, pp. 262–277. https://doi.org/10.1016/B978-0-12-409548-9.11209-6.

Rudels, B., Björk, G., Nilsson, J., Winsor, P., Lake, I., Nohr, C., 2005. The interaction between waters from the Arctic Ocean and the Nordic Seas north of Fram Strait and along the East Greenland Current: results from the Arctic Ocean-02 Oden expedition. J. Mar. Syst. 55, 1–30. https://doi.org/10.1016/j.jmarsys.2004.06.008.

Schaffer, J., von Appen, W.J., Dodd, P.A., Hofstede, C., Mayer, C., de Steur, L., Kanzow, T., 2017. Warm water pathways toward Nioghalvfjerdsfjorden Glacier, Northeast Greenland. J. Geophys. Res. Oceans Res. 122, 4004–4020. https://doi.org/10.1002/2016JC012462.

Schuur, E.A.G., Abbott, B.W., Bowden, W.B., Brovkin, V., Camill, P., Canadell, J.G., Chanton, J.P., Chapin, F.S., Christensen, T.R., Ciais, P., Crosby, B.T., Czimczik, C.I., Grosse, G., Harden, J., Hayes, D.J., Hugelius, G., Jastrow, J.D., Jones, J.B., Kleinen, T., Koven, C.D., Krinner, G., Kuhry, P., Lawrence, D.M., McGuire, A.D., Natali, S.M., O'Donnell, J.A., Ping, C.L., Riley, W.J., Rinke, A., Romanovsky, V.E., Sannel, A.B.K., Schädel, C., Schaefer, K., Sky, J., Subin, Z.M., Tarnocai, C., Turetsky, M.R., Waldrop, M.P., Walter Anthony, K.M., Wickland, K.P., Wilson, C.J., Zimov, S., 2013. Expert assessment of vulnerability of permafrost carbon to climate change. Clim. Chang. 119, 359–374. https://doi.org/10.1007/s10584-013-0730-7.

Schuur, E.A.G., McGuire, A.D., Schädel, C., Grosse, G., Harden, J.W., Hayes, D.J., Hugelius, G., Koven, C.D., Kuhry, P., Lawrence, D.M., Natali, S.M., Olefeldt, D., Romanovsky, V.E., Schaefer, K., Turetsky, M.R., Treat, C.C., Vonk, J.E., 2015. Climate change and the permafrost carbon feedback. Nature 520, 171–179. https://doi.org/10.1038/nature14338.

Semeniuk, D.M., Bundy, R.M., Payne, C.D., Barbeau, K.A., Maldonado, M.T., 2015. Acquisition of organically complexed copper by marine phytoplankton and bacteria in the northeast subarctic Pacific Ocean. Mar. Chem. 173, 222–233. https://doi.org/10.1016/j.marchem.2015.01.005.

Shank, G.C., Whitehead, R.F., Smith, M.L., Skrabal, S.A., Kieber, R.J., 2006. Photodegradation of strong copper-complexing ligands in organic-rich estuarine waters. Limnol. Oceanogr. 51, 884–892. https://doi.org/10.4319/lo.2006.51.2.0884.

Slagter, H.A., Reader, H.E., Rijkenberg, M.J.A., Rutgers van der Loeff, M., de Baar, H.J.W., Gerringa, L.J.A., 2017. Organic Fe speciation in the Eurasian Basins of the Arctic Ocean and its relation to terrestrial DOM. Mar. Chem. 197, 11–25. https://doi.org/10.1016/j.marchem.2017.10.005.

Slagter, H.A., Laglera, L.M., Sukekava, C., Gerringa, L.J.A., 2019. Fe-binding organic ligands in the humic-rich TransPolar Drift in the surface Arctic Ocean using multiple voltammetric methods. J. Geophys. Res. Oceans 124, 1491–1508. https://doi.org/10.1029/2018JC014576.

Søndergaard, J., Mosbech, A., 2022. Mining pollution in Greenland - the lesson learned: a review of 50 years of environmental studies and monitoring. Sci. Total Environ. 812, 152373 https://doi.org/10.1016/j.scitotenv.2021.152373.

Stedmon, C.A., Amon, R.M.W., Rinehart, A.J., Walker, S.A., 2011. The supply and characteristics of colored dissolved organic matter (CDOM) in the Arctic Ocean: Pan Arctic trends and differences. Mar. Chem. 124, 108–118. https://doi.org/10.1016/j.marchem.2010.12.007.

Sunda, W.G., 1989. Trace metal interactions with marine phytoplankton trace metal interactions with marine phytoplankton. Biol. Oceanogr. 6, 411–442.

Sunda, W.G., Lewis, J.A.M., 1978. Effect of complexation by natural organic ligands on the toxicity of copper to a unicellular alga, Monochrysis lutheri. Limnol. Oceanogr. 23, 870–876. https://doi.org/10.4319/lo.1978.23.5.0870.

Thomas, D.N., Lara, R.J., Hajo, E., Kattner, G., Skoog, A., Skoog Alfred Wegener, A., 1995. Dissolved organic matter in Arctic multi-year sea ice during winter: major components and relationship to ice characteristics. Polar Biol. 15, 477–483.

Tovar-Sánchez, A., Duarte, C.M., Alonso, J.C., Lacorte, S., Tauler, R., Galbán-Malagón, C., 2010. Impacts of metals and nutrients released from melting multiyear Arctic sea ice. J. Geophys. Res. 115, C07003 https://doi.org/10.1029/2009JC005685.

Tuerena, R.E., Hopkins, J., Buchanan, P.J., Ganeshram, R.S., Norman, L., Appen, W., Tagliabue, A., Doncila, A., Graeve, M., Ludwichowski, K.U., Dodd, P.A., Vega, C., Salter, I., Mahaffey, C., 2021. An Arctic Strait of two halves: the changing dynamics of nutrient uptake and limitation across the Fram Strait. Glob. Biogeochem. Cycles 35. https://doi.org/10.1029/2021GB006961.

Twining, B.S., Baines, S.B., 2013. The trace metal composition of marine phytoplankton. Annu. Rev. Mar. Sci. 5, 191–215. https://doi.org/10.1146/annurev-marine-121211-172322.

van den Berg, C.M.G., 1982. Determination of copper complexation with natural organic ligands in seawater by equilibration with MnO2 II. Experimental procedures and application to surface seawater. Mar. Chem. 11, 323–342. https://doi.org/10.1016/0304-4203(82)90029-9.

van den Berg, C.M.G., Merks, A.G.A., Duursma, E.K., 1987. Organic complexation and its control of the dissolved concentrations of copper and zinc in the Scheldt Estuary. Estuar. Coast. Shelf Sci. 24, 785–797.

Walsh, M.J., Ahner, B.A., 2013. Determination of stability constants of Cu(I), Cd(II) & Zn (II) complexes with thiols using fluorescent probes. J. Inorg. Biochem. 128, 112–123. https://doi.org/10.1016/j.jinorgbio.2013.07.012.

Walsh, M.J., Goodnow, S.D., Vezeau, G.E., Richter, L.V., Ahner, B.A., 2015. Cysteine enhances bioavailability of copper to marine phytoplankton. Environ. Sci. Technol. 49, 12145–12152. https://doi.org/10.1021/acs.est.5b02112.

Wang, Q., Wekerle, C., Wang, X., Danilov, S., Koldunov, N., Sein, D., Sidorenko, D., Appen, W., Jung, T., 2020. Intensification of the Atlantic water supply to the Arctic Ocean through Fram Strait induced by Arctic Sea ice decline. Geophys. Res. Lett. 47 https://doi.org/10.1029/2019GL086682.

Whitby, H., van den Berg, C.M.G., 2015. Evidence for copper-binding humic substances in seawater. Mar. Chem. 173, 282–290. https://doi.org/10.1016/j.marchem.2014.09.011.

Whitby, H., Hollibaugh, J.T., van den Berg, C.M.G., 2017. Chemical speciation of copper in a salt marsh estuary and bioavailability to Thaumarchaeota. Front. Mar. Sci. 4 https://doi.org/10.3389/fmars.2017.00178.

Whitby, H., Posacka, A.M., Maldonado, M.T., van den Berg, C.M.G., 2018. Copper-binding ligands in the NE Pacific. Mar. Chem. 204, 36–48. https://doi.org/10.1016/j.marchem.2018.05.008.

Williford, T., Amon, R.M.W., Kaiser, K., Benner, R., Stedmon, C., Bauch, D., Fitzsimmons, J.N., Gerringa, L.J.A., Newton, R., Hansell, D.A., Granskog, M.A., Jensen, L., Laglera, L.M., Pasqualini, A., Rabe, B., Reader, H., Rutgers van der Loeff, M., Yan, G., 2022. Spatial complexity in dissolved organic matter and trace elements driven by hydrography and freshwater input across the Arctic Ocean during 2015 Arctic GEOTRACES expeditions. J. Geophys. Res. Oceans 127. https://doi.org/10.1029/2022JC018917.

Wilson, N., Straneo, F., Heimbach, P., 2017. Satellite-derived submarine melt rates and mass balance (2011–2015) for Greenland's largest remaining ice tongues. Cryosphere 11, 2773–2782. https://doi.org/10.5194/tc-11-2773-2017.

Wiwit, Wong, K.H., Fukuda, H., Ogawa, H., Mashio, A.S., Kondo, Y., Nishioka, J., Obata, H., 2021. Wide-range detection of Cu-binding organic ligands in seawater using reverse titration. Mar. Chem. 230, 103927 https://doi.org/10.1016/j.marchem.2021.103927.

Wong, K.H., Obata, H., Kim, T., Kondo, Y., Nishioka, J., 2021. New insights into the biogeochemical cycling of copper in the subarctic Pacific: distributions, size fractionation, and organic complexation. Limnol. Oceanogr. 66, 1424–1439. https://doi.org/10.1002/lno.11695.

Zabłocka, M., Kowalczuk, P., Meler, J., Peeken, I., Dragańska-Deja, K., Winogradow, A., 2020. Compositional differences of fluorescent dissolved organic matter in Arctic Ocean spring sea ice and surface waters north of Svalbard. Mar. Chem. 227, 103893 https://doi.org/10.1016/j.marchem.2020.103893.

Zuehlke, R.W., Kester, D.R., 1983. Copper speciation in marine Waters. In: Trace Metals in Sea Water. Springer US, Boston, MA, pp. 773–788. https://doi.org/10.1007/978-1-4757-6864-0_42.